ADVANCED FUNCTIONAL MATERIALS
www.afm-journal.de

Molecular Insights into [2.2]Paracyclophane-Based Functional Materials: Chemical Aspects Behind Functions

Zahid Hassan

Many of the functions and features of practically useful materials are the province of molecular-level chemistry and their modulation at different length-scale. This report illustrates the molecular-level chemistry behind functions and features of the [2.2]paracyclophane-based materials with a particular focus on the most recent explorations on through-space conjugated small-molecule organic emitters, π-stacked macrocyclic molecules and polymers, poly(p-phenylenevinylene)s featuring well-defined donor-acceptors sequence control, and surface engineering of technologically-relevant parylenes that finds broad applications across the field of chemical science and technology. This report largely deals with the potential and opportunities associated with molecular features and functions of planar chirality, conformational behaviors, strain-induced non-planarity of the aromatics, the profound impacts of through-space conjugation and π-electron interactions/delocalization on optoelectronic properties of the π-conjugated organic emitters, polymers and extended structures consisting of cyclophanes. A special focus is put on the concept of supramolecular polymers using chemically-programmed chiral cyclophanes via non-covalent stacking and controlled conformational arrangements. Illustrating cyclophane as precursors/monomers and fabrication strategies for their incorporation in structurally-controlled (poly(*p*-xylylene)s formed via chemical vapor deposition polymerization and post-deposition fabrication for interface engineering is described. Demonstrating a rather different approach of electronically-dictated ring-opening metathesis polymerization employing strained cyclophane-diene precursors that generate conjugated poly(*p*-phenylenevinylene)s with well-defined (i.e., low dispersity) and donor-acceptor sequence control is also discussed. This report will serve as an indispensable one-stop reference for organic, and polymer chemists, as well as material scientists working with cyclophanes for research innovations.

1. Background and General Overview of the Cyclophane Chemistry

The general term "cyclophane" is coined to name any small or larger cyclic system with or without heteroatoms containing methylene-bridged aromatic ring(s); hence a structurally diverse class of -$[CH_2]_n$-bridged aromatic molecular systems can be referenced as cyclophanes.[1] Each bridge is indicated by a number placed inside a bracket before the cyclophane's name such as [2.2]paracyclophane, [3.3]paracyclophane, or a more general formula of [X]Ycyclophane is used where X inside the brackets denotes the number of bridge(s) constituent atoms in chain(s) and Y in parentheses defines the substitution pattern of the aromatic (core)s. The aesthetically appealing and stereochemically remarkable molecular architecture of cyclophanes, and their unusual reactivities/functions has been of substantial importance from the perspective of fundamental synthetic curiosity to their wide range of applications across the field of chemical science and technology. Our current understanding of cyclophane chemistry, from $[2_n]$cyclophanes to multi-layered cyclophanes, multi-bridged superphanes, and ring-fused or bridge-extended cyclophane systems has been developed through extensive investigations by the pioneering research of D. J. Cram,[2] S. Misumi,[3] J. Nishimura,[4] V. Boekelheide,[5] H. Hopf,[6] A. de Meijere,[7] R. Gleiter,[8] and many others of this era who had devoted significant efforts to the development of new synthesis methods for cyclophane systems which has been the subject of excellent articles, in-depth reviews, book chapters and several patents on applications. This shall not be confused with cycloparaphenylenes which are cyclic all-*para*-linked simple string of phenyl rings (and have no aliphatic bridges).[9] Some of the representative prototypical cyclophanes are depicted in **Figure 1**.

In 2004, an extensive monograph "Modern Cyclophane Chemistry" edited by H. Hopf and R. Gleiter was published by Wiley-VCH.[10] This landmark monograph consisting of twenty chapters by a diverse spectrum of prominent experts presents historical aspects of cyclophanes chemistry ranging from synthetic

Z. Hassan
Institute of Organic Chemistry (IOC)
Karlsruhe Institute of Technology (KIT)
Fritz-Haber-Weg 6, 76131 Karlsruhe, Germany
E-mail: zahid.hassan@kit.edu
Z. Hassan
Material Research Center for Energy Systems (MZE)
Strasse am Forum 7, Bldg. 30. 48, 76131 Karlsruhe, Germany
The ORCID identification number(s) for the author(s) of this article can be found under https://doi.org/10.1002/adfm.202311828

DOI: 10.1002/adfm.202311828

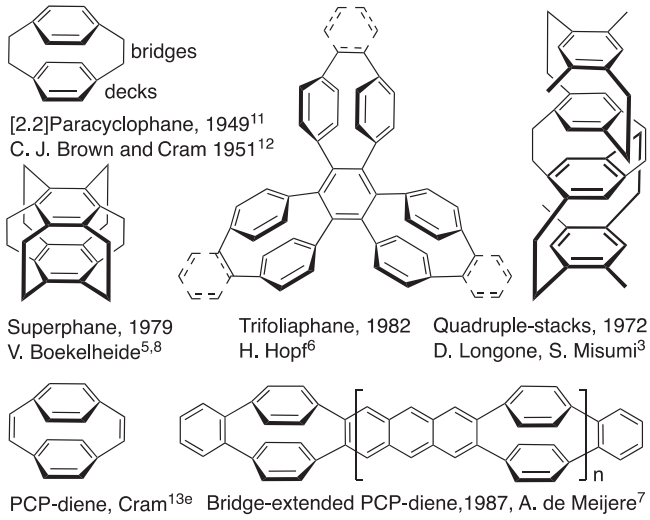

Figure 1. Prototypical cyclophanes: [2$_n$]cyclophanes, multi-bridged superphanes, multi-layered cyclophanes, and bridge-extended cyclophane homologue π-systems.

curiosity to mechanistics, demonstrating structure/reactivity relationships and understanding their unusual physicochemical properties. In recent years, however the cyclophane chemistry has evolved from functional molecules to functional materials as witnessed by the dramatic increase in the breakthrough research and number of scientific publications frequently appear in most prestigious academic journals of chemical sciences. The subject and title of this report "Molecular Insights into [2.2]Paracyclophane-based Functional Materials: Chemical Aspects Behind Functions" highlights the new paradigms with a special focus on technologically-relevant functional materials formed from chemically-programmed cyclophane-based molecular precursors.

2. Repurposing [2.2]Paracyclophanes as Modular Precursors for Materials Fabrication

C. J. Brown and A. C. Farthing first discovered PCP in 1949 by the gas-phase pyrolysis of *p*-xylene at low-pressure "Preparation and Structure of Di-*p*-Xylylene" using the technique described by Szwarc.[11] 2 years later in 1951, the first synthesis of paracyclophanes was reported by D. J. Cram and H. Steinberg from 1,4-bis(bromomethyl)benzene by intramolecular Wurtz cyclization reaction.[12] D. J. Cram suggested the name "Paracyclophane" for this class of compounds. [2.2]Paracyclophane or [2.2](1,4)cyclophane is abbreviated as PCP (other term such as pCp, and PC are also referred to the [2.2]paracyclophane). PCP is the smallest stable co-facially stacked pro-chiral 3D strained scaffold where two benzene rings are rigidly held in a face-to-face orientation by two short ethylene bridges -[CH$_2$]$_2$- in their *para*-positions which has been investigated by Donald Cram, and many others for decades (for details about the pioneering research on [2.2]paracyclophanes, see ref. [13]) The co-facial stacking of the two benzene rings in PCP (with short inter-ring distances between ≈2.83 and 3.09 Å in decks) causes a distortion and transannular π—π electronic interaction that provide the basis for unique physicochemical characteristics of the PCP molecules (for detail discussion about the structural chemistry and metrical data of the [2.2]paracyclophane, see ref. [14]). As a result of steric hinderance, the two benzene rings in PCP are slightly bent out of planarity accompained by a corresponding up-and-down movements of the methylene bridges; and twisted by ≈6° in their planes relative to one another. PCP derivatives provide a promising platform to study the element of planar chirality as PCP exhibits unique stereochemical features (planar chirality) on selective functionalization. PCP belongs to the D_{2h} point group, which is broken by the first substituent, resulting in planar chiral enantiomers. The stereochemical notations R_p-, and S_p- define the planar chirality of the PCP enantiomers according to the Cahn Ingold-Prelog (CIP) system which is present in [2.2]paracyclophane derivatives.

It is important to mentioned that one of the most fundamental and principal aspects of [2.2]paracyclophane chemistry is the development of planar chiral ligand/catalyst systems which proved to be useful toolbox for stereo-controlled synthesis.[15] For instance, PCP-derived PhanePhos being one of the most prominent example of planar chiral ligands employed in diverse synthetic transformations shows that planar chirality is a viable alternative to the most conventional central/point chirality and offers new opportunities for the development of efficient ligand/catalyst systems.[16] Although compared to ferrocene ligands (like JosiPhos family that contain two individual crucial features; planar chirality in addition to point chirality which has been a prerequisite for high reactivity/enantioselectivity), PCP-based ligands/catalysts are rarely explored. Diverse applications of PCPs as chiral ligands or catalysts in a wide range of asymmetric syntheses investigated by the research groups of Rozenberg,[17] Rowlands,[18] Paradies,[19] Micouin and Benedetti,[20] Ma,[21] Bolm,[22] Bräse,[23] Zhou and colleagues[24] have been well-documented in literature. An in-depth survey of the planar chiral ligands and catalysts is beyond the mandate of this report.

To build synthetic molecules and studying their properties is a broad area of research in itself. However, transforming small molecules into practically useful materials through ensuing interdisciplinary research at the chemistry-materials interface is even more rewarding to harvest the multifold potential of synthesis from fundamental explorations to emerging applications. From the perspective of synthetic planning and function-led design considerations of materials, everything starts with molecular building blocks that bring desired functions and features once incorporated into materials. The functions and features of a synthetic material can arise from precursors formulations, their compositional variation, and controlled fabrication at different length-scales by employing various fabrication methods and techniques.

Considering the interesting molecular feature/aspects of the PCPs make them useful precursors in materials fabrication. Using carefully chosen synthesis routes, different functional groups can be selectively attached at the ethylene bridges -[CH$_2$]$_2$- or either benzene rings that is, mono-, and/or multiply substituted-PCP regioisomers including pseudo-*para*, -*ortho*, -*meta*, and -*gem* derivatives can be synthesized to serve a particular purpose in materials fabrications. The colloquial nomenclature is

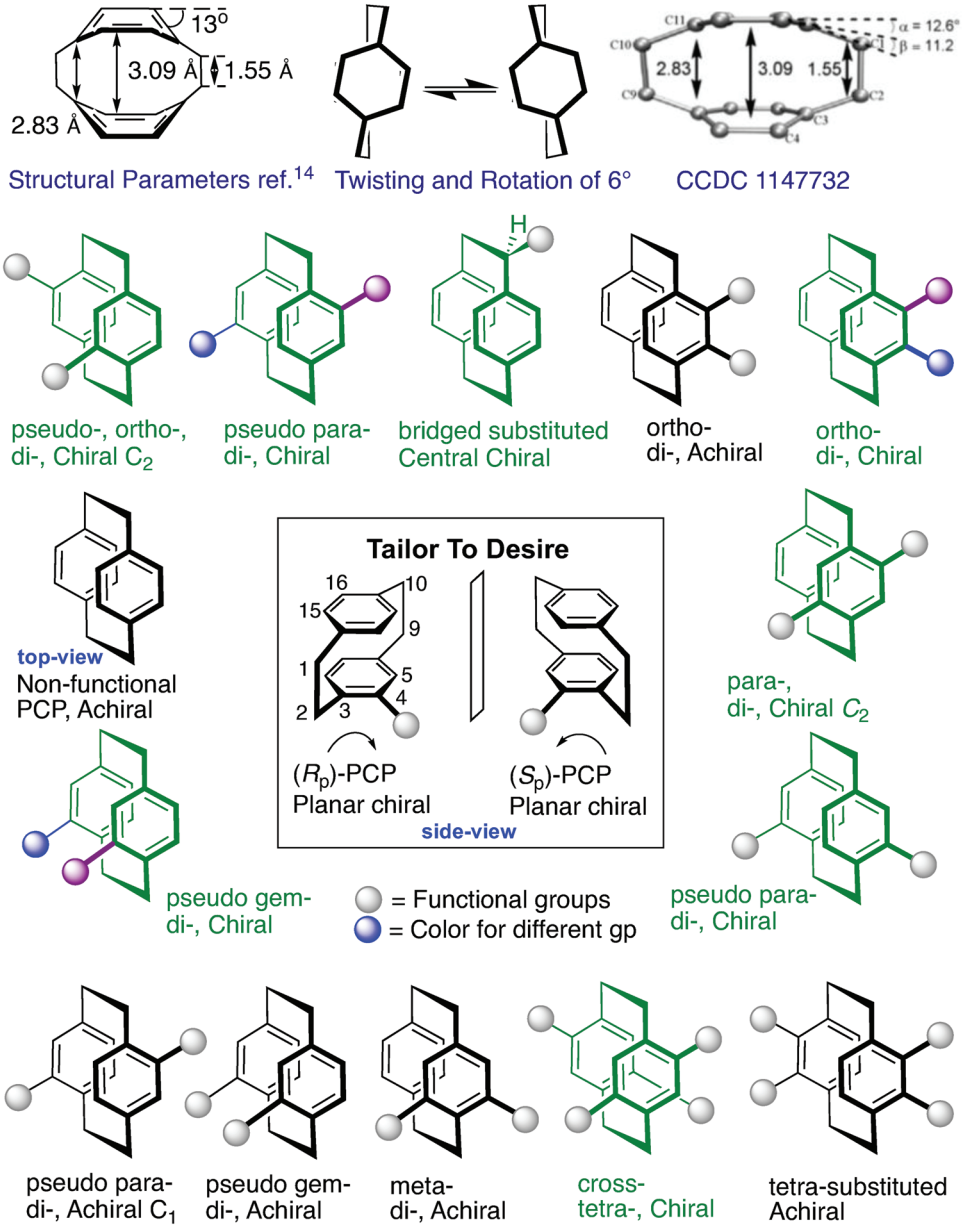

Figure 2. Structural parameters of the PCP adopted from X-ray crystal structure (CCDC1147732) ref. [14] and the conformational interconversion of the two equivalent D_{2h} conformers (top); Common substitution patterns of mono-, di-, and tetra-substituted PCPs with stereochemical descriptions. Some of this material appeared in the author earlier work ref. [35] Copyright 2020 Wiley-VCH.

self-evident: for disubstitution on one phenyl ring of the PCP, the conventional prefixes of *ortho-*, *meta-*, and *para-* are used, while disubstitution on two transannularly adjacent positions on the benzene rings gives rise to pseudo-*geminal*, pseudo-*ortho*, pseudo-*meta*, and pseudo-*para* prefixes to specify *ortho-*, *meta-*, and *para-* relationships displaced from the usual homoannular into a transannular context. The diverse synthetic approaches developed so far cannot be reviewed in a short synopsis because of the immense structural and functional diversity of the PCP. For some know-how of the PCP chemistry, an overview of the most common mono-, di-, and tetra-substituted PCPs along with stereochemical description is presented in **Figure 2**.

2.1. Design Strategies, Skeletal Composition, and Functionalization of the PCP Scaffolds as Modular Precursors

Chemists can synthesize a range of building blocks that are readily assembled to form function-inspired materials like interlocking Lego bricks can be assembled to construct an array of objects. The modular nature of the PCP core offers a chemically-programmable scaffold. By incorporating multiple small molecular fragments together in a single customized PCP unit, where each fragment is intended to serve a particular purpose, make them attractive synthons from the perspective of their applications in functional materials. To serve a particular purpose,

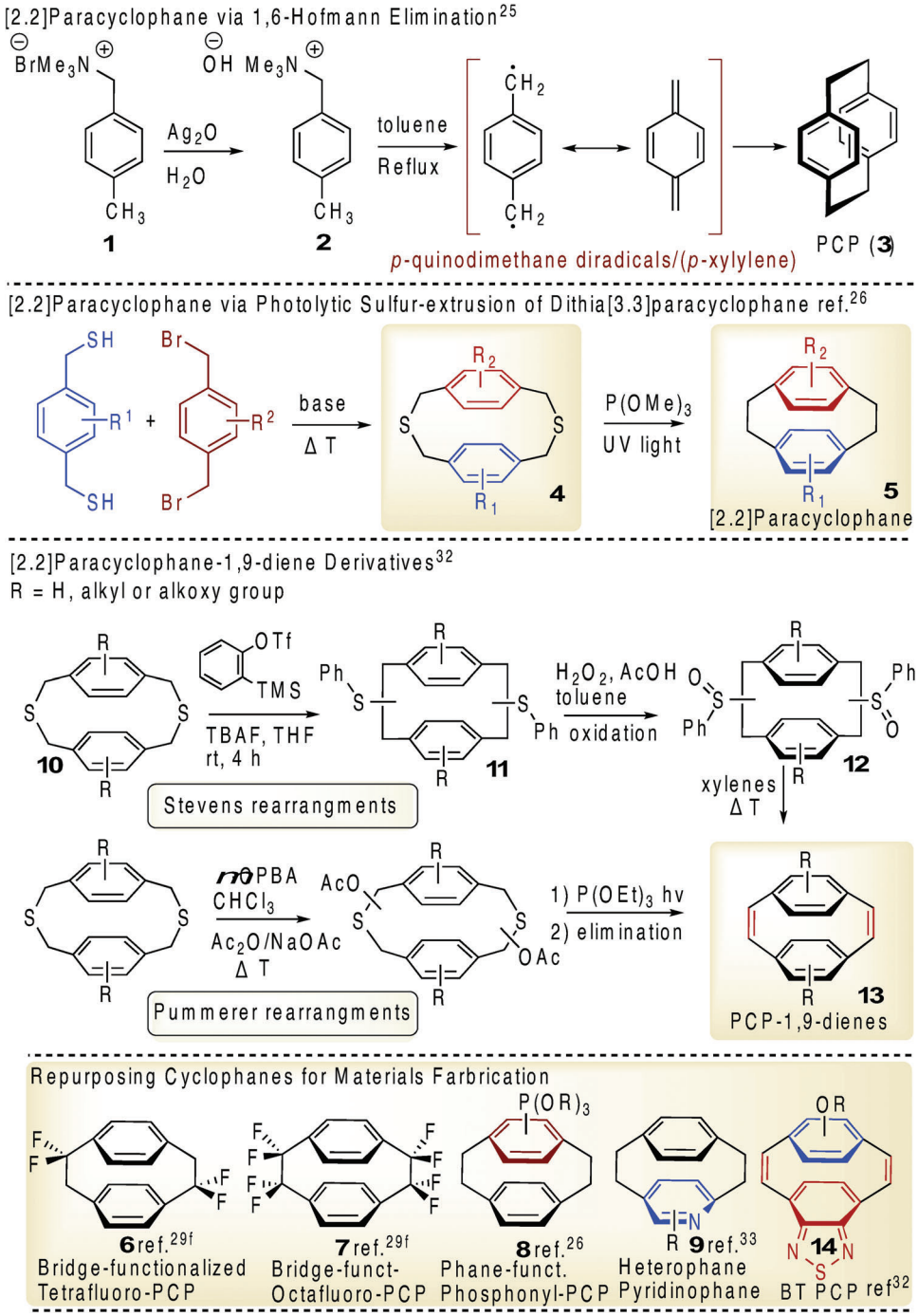

Scheme 1. General synthesis strategies of PCP via 1,6-Hofmann elimination-dimerization of quaternary ammonium salts, and functionalized PCPs by annulation/sulfur extrusion approach and synthesis of PCP-dienes through Stevens/Pummerer rearrangments.

backbone composition of the PCP, that is, both at the arene and/or ethylene bridges can be fine-tuned to access functionalized PCPs.

PCP can be prepared based on the Hofmann elimination reaction of a *p*-methylbenzyltrimethylammonium hydroxide (via quinodimethane intermediate).[25] By the addition of silver(I) oxide to the ammonium salt (*p*-methylbenzyltrimethylammonium bromide (**1**), the corresponding ammonium hydroxide intermediate (**2**) is generated which upon heating form *p*-xylylene. This *p*-xylylene is in resonance with a diradical that dimerizes to give PCP (**3**). This route is quite low-yielding (17%). One of the well-known synthesis methods of PCP is using dithia[3.3]paracyclophane derivatives (**4**) which is formed from two aromatic analogs of 1,4-bis(mercaptomethyl)benzene and 2,5-dibromo-*p*-xylene (**Scheme 1**). On sulfur-extrusion, dithia[3.3]paracyclophanes give access to the corresponding PCP

derivatives (**5**).[26] This method is particularly suitable to access PCPs with functionalization at the aliphatic bridges or to access disparately substituted arene decks of the PCP. Other facile route to prepare (hetera)cyclophanes has also been developed using dithiols in combination with a pnictogen additive in the presence of iodine (metalloid-directed self-assembly method that generate disulfides, thioethers and sulfones).[27] Treatment of the corresponding disulfide-bridged (hetera)cyclophanes with hexamethylphosphorous triamide generate thiacyclophanes. The thiacyclophanes by treatment with triethylphosphite $P(OEt)_3$ under UV-light irradiation generate sulfur-extruded cyclophanes. Using this approach, 4,5,7,8-tetrafluoro- and 4,5,7,8,12,13,15,16-octafluoro-PCP can be prepared with fluoro-substitution at either one or both benzene rings of the PCP core.[28]

The alkyl hydrogen atoms of the two ethylene bridges -$[CH_2]_2$- in PCP can be functionalized either fully or partially by substituting fluorine atoms to generate 1,1,9,9-tetrafluoro-PCP, or 1,1,10,10-tetrafluoro-PCP (**6**), and 1,2,9,10-octafluoro-PCP (**7**).[29] The bridge-fluorinated PCP, called AF4, is one of the most useful precursor of particular commercial interest used in parylene-AF4 polymeric coating formed by cyclophane-based chemical vapor deposition polymerization (CVD). Polymers formed from fluoro-PCP represent high thermal and chemical stabilities. 1,9- and 1,10-dibromodienes can be obtained from a mixture of the 1,1,9,9- and 1,1,10,10-tetrabromo-PCP by dehydrobromination with potassium tert-butoxide (*tert*-BuOK) in tert-butyl methyl ether (MTBE). Subsequent addition of Br_2 gave a mixture of the hexabromides, which upon dehydrobromination (*tert*-BuOK, MTBE) generate 1,2,9,10-tetrabromo[2.2]paracyclophanediene.[30] The bromination of the two isomeric tetrafluoro-PCP enable mono- and dibromination of 1,1,9,9-tetrafluoro-PCP in high yields.

In a similar way, [2.2]paracyclophane-1,9-diene (PCP-d), contain two strained carbon–carbon double bonds "vinylene bridges" joining the two aromatic rings "decks" in their *para*-positions. Due to the high inherent strain, PCP-d derivatives are emerged among the most investigated class of cyclophanediene as monomer in the living ring opening metathesis polymerization (ROMP) process for the synthesis of poly(*p*-phenylenevinylene)s (PPV)s polymers as first reported in 1992 by Thorn–Csányi.[31] The PCP-d and certain derivatives are prepared from dithia[3.3]paracyclophane derivatives (**10**) which involved a benzyne-induced Stevens rearrangement (BSR) or Pummerer rearrangments via a dithiacyclophane ring contraction to access the corresponding bis(sulfide)-PCP (**11**).[32] Subsequent oxidation gives access to the PCP bis(sulfoxide) (**12**) followed by thermal *syn*-elimination step afford the desired PCP-d derivatives (**13**). The BSR route generally yields low quantities of the desired PCP-d, whereas the Pummerer rearrangement offers improved yields. The BSR of dithiacyclophane is performed by the slow addition of TBAF·$3H_2O$ to a THF solution of 2-(trimethylsilyl)phenyl trifluoromethanesulfonate as the benzyne source to prepare PCP-d with alkyle side chains (ultimately alkyl substituted PPVs by ROMP).

Although PCP scaffolds are widely restricted to simple all-carbon backbones. By replacing one or both benzene rings with heteroaromatics, skeletally novel scaffolds consisting of two varying constituent units such as pyridinophane derivatives (**9**) can be prepared as useful precursor components.[33] To form an unsymmetric donor–acceptor benzothiadiazole-PCP-d, an electron-deficient aromatic heterocyclic core of benzothiadiazole together with (4-methoxy-1-(2-ethylhexyl)oxy)-benzene as electron-donating ring can be incorporated into cyclophane (**14**).[34] The skeletal and functional composition of the PCP-d can influence the properties of the resulting ROMP-based PPVs polymers.

Recent advances in synthetic approaches toward regioselective functionalization of the PCP scaffolds,[35] and their useful utility as chemically-programmed precursors in polymers and materials fabrication have been reviewed in inspiring focused reports.[36] The upcoming sections summarize details to showcase the useful utility of some customized PCPs as useful precursors/monomers and strategies for their incorporation into functional systems are described.

3. [2.2]Paracyclophane-Based Through-Space Conjugated π-Stacked Chiroptical and Optoelectronic Materials

One of the most recent focuses of PCP-derived systems centers on technologically-relevant optoelectronic material applications dealing with strain-induced non-planarity, conformational behavior, through-space conjugation, and π-electron interactions/delocalization as decisive factors in tuning optoelectronic properties and functions.[37] The characteristics of rigid skeleton, chemical and photo stability, planar charity, and through-space electronic communication possessed by the PCP core make it a useful building block for organic semiconductor materials. Through-space conjugation is an important way of π-electron interactions/delocalization within closely stacked π-systems in parallel with the conventional intramolecular charge transfer processes through-bond path. Understanding the role of intermolecular interactions and quantifying through-space charge transfer in π–stacked molecular systems is central to the rational design of organic electronic materials.[38] Guillermo Bazan and colleagues have comprehensively investigated PCP-derived phenylenevinylenes (PCP functionalized with donor (D) and/or acceptor (A) stilbenoid dimer-type bichromophoric systems) to examine the influence on the optical and electronic properties of the chromophores components as a function of their structure/property spatial relationship. Bazan in his several *Accounts* has reviewed this topic that provides a comprehensive overview.[39] The PCP skeleton serves as the locus of interchromophore contact and the varying spatial arrangements (geometric relationships) allows to bring chromophores together into close proximity. Chemical and spectral evidence indicates the presence of strong transannular electronic interactions in PCP and its derivatives. The absorption maximum of vinylphenyl-PCP (λ_{abs} = 318 nm) and of noncyclophanyl stilbene (λ_{abs} = 294 nm) provides the first indication of the influence of stacking phenylene units in PCPs. The chromophores conjugation length at specific distances, and their orientation relative to one another (modulated via regiochemistry of ps-*ortho*-, ps-*meta*-, and ps-*para*- substitutions on PCP) have critical effects in defining the optoelectronic functions. For instance, with four-fold donor and acceptor substitution at the carbon atoms 4-, 7-, 12-, and 15-position of the PCP were studied to probe the phenomenon of delocalization (spatial/through-space charge transfer) on the nonlinear optical properties.[40] Higher photoluminescence quantum

efficiencies and more red-shifted emission for the cyclophanyl species bearing extended conjugation were observed. Through-space delocalization across the PCP core is more polarizable in the excited state, relative to the through-bond excited state. When strong donors are attached to the distyrylbenzene chromophore, the charge transfer character of the distyrylbenzene-based excited state dominates fluorescence properties. This work on PCP-derived molecular systems demonstrates how well-defined organic molecules can be used as study models to unravel complex phenomena in optical and electronic materials.

3.1. π-Stacked Small-Molecule Organic Emitters consisting of Optically Active [2.2]Paracyclophanes

Organic light emitting diodes (OLED)s has been widely used as one of the most promising electroluminescent technologies in a range of applications, such as smartphones, high-resolution screens and digital displays.[41] By avoiding the use of costly metal-based phosphorescent molecules used in electroluminescent materials that trigger environmental contamination concerns, researchers aim to develop organic structures that emit colorful light with high efficiency, color purity and easy synthetic access. Addressing the efficiency and stability issues associated with fluorescent materials, a major milestone was achieved by Adachi and colleagues in 2012 by developing a new class of metal-free organic electroluminescent TADF emitters (contain multiple carbazolyl dicyanobenzene derivatives; CzIPN).[42] TADF is the recent breakthrough and most promising exciton harvesting mechanism. TADF emitters design call for minimizing non-radioactive decay, rigid-structures that have a strongly twisted donor-acceptor (D–A) wherein the electron density in the highest occupied molecular orbital (HOMO) is mainly localized on the donor moiety while the lowest unoccupied molecular orbital (LUMO) is found on the electron-withdrawing acceptor leading to a small exchange integral and thus reduce the energy difference between its singlet (S_1) and triplet (T_1) excited states (ΔE_{ST}) maintaining a high electroluminescence efficiency. When (ΔE_{ST} is <0.1 eV, thermal upconversion from T_1 to S_1 state by reverse intersystem-crossing (RISC) becomes possible.[42b]

PCP-based donor/acceptor-type small-molecules are considered promising candidates as stable, efficient, blue-light emitting compounds for OLEDs applications.[43] Enantiopure PCP component impart planar chirality, and emissive analogs can exhibit circularly polarized luminescence (CPL).[44] CPL is one of the optical properties of chiral systems that measures the intensity difference between the left- and right-circularly polarized emission from an intrinsically chiral material. For evaluating the performance of CPL-active materials luminescence dissymmetry factor (g_{lum}), that is, the relative intensity difference of left and right circularly polarized absorption (in CD) or emission (in CPL), and quantum yield (Φ_F) are critical parameters. Fluorescence intensity, wavelength, and degree of dissymmetry of small chiral organic molecules can be modulated through their structural modifications for practical applications. In 2018, Bräse, Zysman-Colman and colleagues introduced the first examples of through-space conjugated TADF emitters based on a PCP skeleton (**15**). Their optoelectronic properties were studied by the relative configuration of pseudo-*geminal* and pseudo-*para* of the donor and acceptor groups substituted on PCP. Decorating both decks of the PCP selectively (pseudo-*gem* and pseudo-*para*) with electron-donor and acceptor units allowed intramolecular charge transfer (ICT) through the π-stacked PCP core.[45] The coplanar stacked donor and acceptor groups exhibit promising optoelectronic properties depending on their relative orientation of PCP-derivatives (**Figure 3**). (4′-*N*,*N*-diphenylamino)phenyl and (4′-*N*-carbazolyl)phenyl as donors and benzoyl acceptor group (varying in their regiochemistry), that is, pseudo-*gem* and pseudo-*para*-Bz-PCP-TPA isomers showed blue TADF emission with photoluminescence maxima (λ_{PL}) at 480 and 465 nm in doped films (15 wt% mCP), with yet low photoluminescence quantum yields (Φ_{PL}) of 12% and 15% in the solid state. Electronic communication between donor and acceptor groups on adjoining benzene decks facilitates the separation of HOMO and LUMO and thus results into TADF.

Later, Zhao and colleagues have reported a new family of solid-state emissive triarylborane-based PCP-derivatives (**16**) of pseudo-*gem*-$BNMe_2$-PCP and pseudo-*meta*-$BNMe_2$-PCP displaying intense circularly polarized luminescence and thermally activated delayed fluorescence.[46] This scaffold contains dimesitylboryl $BMes_2$ (as bulky electron-withdrawing group) and NMe_2 (as electron-donating group) at the pseudo-*gem* and pseudo-*meta* positions at two different phenyl rings of the PCP. The centroid–centroid distances between two deck benzene rings of PCP are 3.08 Å for pseudo-*gem*-$BNMe_2$-PCP and 3.01 Å for pseudo-*meta*-$BNMe_2$-PCP, which allows the efficient through-space charge-transfer transitions. A big structure difference between these two compounds is that the nitrogen center in pseudo-*gem*-$BNMe_2$-PCP is more coplanar with the amino-bonded benzene ring than pseudo-*meta*-$BNMe_2$-PCP as determined by X-Rays crystallography. The dihedral angles between NC_3 plane and the NMe_2-bonded benzene ring are 21.8° and 36.8°, respectively. Through-space charge transfer enables the intense fluorescence with TADF characteristics. The quantum yields of the two regioisomeric scaffolds are up to 0.72 (pseudo-*gem*-$BNMe_2$-PCP) and 0.39 (pseudo-*meta*-$BNMe_2$-PCP) in cyclohexane. To explore the chiroptical properties, its enantiomerically pure forms were also prepared. Intense solid-state fluorescence was also observed for the enantiopure pseudo-*gem*-$BNMe_2$-PCP (Φ_F = 0.68 for R_p-isomer; 0.59 for S_p-isomer). The R_p enantiomer displays a small positive signal ≈393 nm and a large positive signal ≈313 nm. The enantiomerically pure forms of pseudo-*gem*-$BNMe_2$-PCP exhibit strong CPL signals with a g_{lum} up to 4.24×10^{-3} (in toluene). This approach was further extended by Zhao and colleagues and introduced a 2-(dimesitylboryl)phenyl ($BMes_2$) containing PCP-derivatives (**17**) of pseudo-*gem*-$BPhNMe_2$-PCP and pseudo-*meta*-$BPhNMe_2$-PCP which contain a phenylene spacer between the PCP and the acceptor moiety.[47] All of the compounds were characterized by the highly pyramidal geometry of nitrogen center (the sum of C—N—C ranging from 343.2° to 352.6°) despite the complete planar geometry of boron center as determined by X-ray crystal structure. The boryl-bonded phenyl ring (P3) is greatly twisted from the neighboring phenyl ring (P2) with the dihedral angles larger than 60°. In addition, there exist π—π stacking interactions between P2 and the phenyl ring (P4) of the mesityl lying over P2, as evidenced by the small dihedral angle (20.3°–24.5°) and the short centroid–centroid distance (3.69–3.78 Å) between them. This small structure change causes a significant increase

π-Stacked Small-molecule Organic Emitters

The Design of New Functions via Through-space Interactions

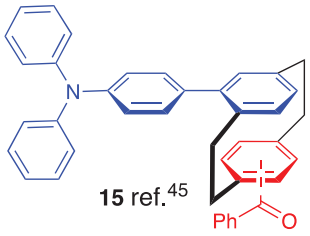

15 ref.[45]

ps-*g*-Bz-PCP-TPA I ps-*p*-Bz-PCP-TPA
ΔE_{ST} = 0.13 eV, 0.17 eV
τ_d = 1.8 ms, 3.6 ms (15 wt% mCP)
λ_{PL}= 480 nm, 465 nm (15 wt% mCP)
Φ_{PL}= 12%, 15% (toluene)

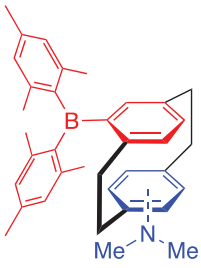

16 ref.[46]

ps-*g*-BNMe$_2$-PCP I
ps-*m*-BNMe$_2$-PCP
ΔE_{ST} = 0.17 eV, 0.12 eV
τ_d = 0.38 ms, 0.22 ms (toluene)
λ_{PL}= 531 nm, 521 nm (toluene),
Φ_{PL}= 72%, 39% (cyclohexane)
$|g_{lum}|$ = 4.2×10^{-3} (toluene), n.a.

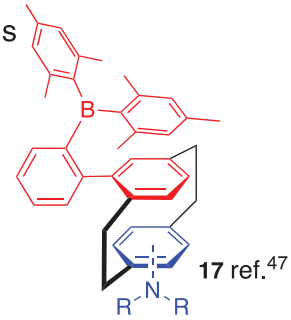

17 ref.[47]

ps-*g*-BPhNMe$_2$-PCP (R=Me)I
ps-*m*-BPhNMe$_2$-PCP (R=Me) I
ps-*m*-BPhNPh$_2$-PCP (R=Ph)
ΔE_{ST}= n.a, τ_d = n.a.
λ_{PL}= 488 nm, 461 nm, 455 nm (C_6H_{12})
Φ_{PL}= 83%, 93%, 82% (cyclohexane)
$|g_{lum}|$ = 1.3×10^{-2},1.7×10^{-2}, 1.7×10^{-2} (THF)

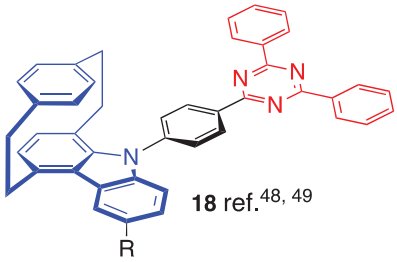

18 ref.[48, 49]

CzpPhTrz (R=H) I CNCzpPhTrz (R=CN) I
CF$_3$CzpPhTrz (R=CF$_3$)
ΔE_{ST} = 0.30 eV, 0.23 eV, 0.22 eV
τ_d = 65 ms (10 wt% DPEPO), 135 ms, 158 ms (10 wt% PPT)
λ_{PL}= 482 nm (10 wt% DPEPO), 458 nm, 456 nm (10 wt% PPT)
Φ_{PL}= 69% (10 wt% DPEPO), 65%, 70% (10 wt% PPT)
$|g_{lum}|$ = 1.3×10^{-3}(toluene), n.a., n.a.
λ_{EL}= 480 nm, 456 nm, 460 nm
EQE$_{max}$ = 17%, 7.4%, 12%

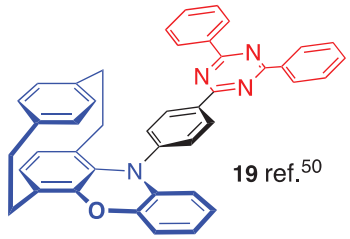

19 ref.[50]

PXZ-PCP-TRZ
ΔE_{ST} = 0.03 eV
τ_d = 12 ms, (10wt% CBP)
λ_{PL}= 548 nm (toluene)
Φ_{PL}= 60% (neat)
$|g_{lum}|$ = 3.3×10^{-3} (toluene)
λ_{EL}= 560 nm, EQE = 7.8%, $|g_{EL}|$= 4.6×10^{-3}

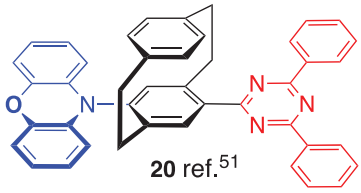

20 ref.[51]

ps-*p*-PXZ-PCP-PT
ΔE_{ST} = 0.19 eV
τ_d = 75 ms, (10 wt% CBP)
λ_{PL}= 565 nm (toluene)
Φ_{PL}= 78% (10 wt% CBP)
$|g_{lum}|$ = 1.9×10^{-3} (toluene)
λ_{EL}= 557 nm, EQE = 20%, $|g_{EL}|$= 1.5×10^{-3}

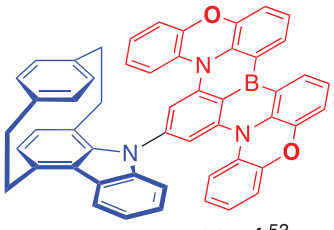

21 ref.[53]

Czp-POAB
ΔE_{ST} = 0.13 eV
τ_d = 62 ms (8 wt% 2,6DCzPPy)
λ_{PL}= 498 nm (toluene)
Φ_{PL}= 96% (8 wt% 2,6DCzPPy)
$|g_{lum}|$ = 4.8×10^{-4} (toluene), 1.4×10^{-3} (2,6DCzPPy)
λ_{EL}= 513 nm, EQE = 29%, $|g_{EL}|$ = 1.3×10^{-3}

Figure 3. Chemical scaffolds, photophysical and OLED applications based on PCP-based small-molecule TADF/CPL emitters and exploring donor–acceptor modification strategy.

in both Φ_F and g_{lum}. In toluene, the Φ_F and g_{lum} of pseudo-*gem*-BPhNMe$_2$-PCP were increased to 0.59 and 1.08 × 10^{-2}, respectively. 2-(Dimesitylboryl)phenyl-substituted PCPs (pseudo-*meta*-BPhNMe$_2$-PCP) have shown intense CPL combing high fluorescence efficiency (Φ_F) and luminescence dissymmetry factor (g_{lum}) up to 0.93 and 1.73 × 10^{-2}, respectively.

In further optimization by the incorporation of an annelated chiral carbazolophane (Czp) as an electron-donor combined with triazine-containing (TRZ) scaffold (**18**) showed a small ΔE_{ST} of 0.16 eV, and λ_{PL} at 480 nm with Φ_{PL} of 70% in 10 wt% bis[2-(diphenylphosphino)phenyl] ether oxide (DPEPO)-doped films.[48] Carbazolophane (indolo[2.2]paracyclophane) adopts a more twisted conformation in donor–acceptor systems due to its larger size compared to the reference non-cyclophanyl emitter. The presence of the PCP induces a torsion of 55.86 Å between the planes of the Czp donor and the phenyl bridge while the corresponding torsion in CzPhTRZ is significantly shallower at 45.11 Å. The distance between decks in the PCP core is 3.07 Å at the N-connected carbon atom, which is consistent with distances in both the free carbazolophane18 (3.06 Å) and non-substituted PCP (3.08–3.10 Å). The increased steric bulk of the annelated donor unit forces an increased torsion between the carbazole and the aryl bridge resulting in a decreased ΔE_{ST} and an enhancement of the TADF. The closely stacked carbazole and benzene units of the PCP show through-space π—π interactions, effectively increasing the spatial occupation for the HOMO orbital. Enantiomeric emitters R_p-, and S_p- were prepared to study CPL properties. The chiroptical properties of enantiomers of the PCP reveal mirror image circular dichroism (CD) and CPL with g_{lum} of 1.3 × 10^{-3}. Sky blue-emitting OLEDs were fabricated with the new TADF emitter showing a high maximum EQE of 17% with CIE coordinates of (0.17, and 0.25).

The functional composition influences the nature of the TADF properties and even minor changes can alter its properties significantly. By the incorporation of electron-withdrawing cyano (CN) and trifluoromethyl (CF_3) groups onto the Czp moiety, two deep-blue TADF emitters namely; CNCzpPhTRZ and CF_3CzpPhTRZ were further developed.[49] The DFT calculations reveal that the frontier orbitals and states are effectively tuned via the introduction of electron-withdrawing groups. The HOMO is located primarily on the carbazolophane donor moiety, while the LUMO is distributed across the triazine acceptor and phenylene bridge. The HOMO levels of the two derivatives are expectedly significantly stabilized at −5.91 eV (CNCzpPhTRZ), and −5.78 eV (CF_3CzpPhTRZ) compared to that of the parent emitter CzpPhTRZ (−5.54 eV) due to the presence of the electron-withdrawing CN and CF_3 groups, respectively. CNCzpPhTRZ and CF_3CzpPhTRZ emits at 458 and 456 nm with Φ_{PL} values of 65 and 70% in 10 wt% 2,8-bis(diphenylphosphoryl)dibenzo[*b*,*d*]thiophene (PPT)-doped film, respectively. Both emitters show high photoluminescence quantum yield. The ΔE_{ST} is 0.23 eV for CF_3CzpPhTRZ and 0.22 eV for CNCzpPhTRZ with long-delayed lifetime of 158.3 µs for CF_3CzpPhTRZ and 135.0 µs for CNCzpPhTRZ in 2,8-bis(diphenyl-phosphoryl)-dibenzo[b,d]thiophene (PPT) host shows TADF behavior. Blue OLEDs exhibited an external quantum efficiency (EQE_{max}) of 7.4% at 456 nm for CNCzpPhTRZ and an EQE_{max} of 11.6% at 460 nm for CF_3CzpPhTRZ. In each of these TADF emitters, only a single deck of the PCP was investigated.

By combining a bulkier phenoxazine (PXZ) donor (called phenoxazinophane; PXZ-PCP on attachment to the planar chiral PCP) and 2,4,6-triphenyl-1,3,5-triazine (TRZ) acceptor enables efficient luminescence performances and excellent CPL properties. The generated molecule PXZ-PCP-TRZ (**19**) possesses a smaller energy difference (ΔE_{ST}) of 0.03 eV between singlet and triplet demonstrating the RISC process is fast leading to yellow TADF properties with an EQE_{max} up to 7.8%. The CP-OLED shows a circularly polarized electroluminescence signals with a g_{EL} up to 4.6 × 10^{-3}.[50] The planar chiral PCP not only enhances the electron delivery ability of phenoxazine through the intramolecular π—π interactions but also enlarges dihedral angle between donor and benzene ring, which has been a critical factor for TADF molecules in lowering the ΔE_{ST} for efficient reverse intersystem crossing.

The PCP-based chiral carbazole (**18**) phenoxazine (**19**) racemized at the temperature of the vacuum deposition, thus further improvement in the racemization barrier of the PCP-based circularly polarized thermally active delayed fluorescence (CP-TADF) emitters were required for device fabrications. To serve this particular purpose, a pair of donor-chiral π-acceptor-type planar chiral TADF emitter *S*-PXZ-PCP-PT (**20**) functionalized with phenoxazinophane donor and triazine acceptor onto the PCP were studied. This not only restrains the racemization caused by the rotation of the sigma bond, making it possible to fabricate CP-OLEDs through the vacuum-deposited processing, but also suppresses the non-radiative transition process to achieve a high photoluminescence quantum yield of 0.78.[51] By integrating a chiral PCP into the luminescent scaffold enable achieving an intense CPL signal with a g_{lum} of 1.9 × 10^{-3} in toluene. The vacuum-deposited CP-OLEDs acquired a high EQE_{max} of up to 20.1% and a g_{EL} of 1.5 × 10^{-3}. Due to the large steric hindrance, the critical torsion between the PXZ donor and the phenyltriazine (PT) acceptor was guaranteed to have high twists with a dihedral angle of 60.2° which results into the larger energy gap of the singlet and triplet (ΔE_{ST}). The vacuum-deposited CP-OLEDs with *R*-(PXZ-PCP)-PT exhibited a yellow emission [(λ_{EL} of 557 nm, CIE of (0.44, 0.55)] with an EQE_{max} of 20.1%. To test the racemization energy barrier of enantiomeric emitter, the *S*-(PXZ-PCP)-PT was boiled in diethylene glycol dibutyl ether at 200 °C for 20, 40, 60 min, the enantiomer was completely free of racemization.

Multi-resonant TADF (MR-TADF) emitters based on the boron/nitrogen (B/N) containing scaffolds are emerging candidates for efficient and color-pure circularly polarized OLEDs.[52] In 2023, Zheng and colleagues introduced a B/N doped PCP-based multiple resonance TADF system (**21**) bearing highly rigid structures composed of carbazole and phenoxazine groups arranged in a specific pattern with boron on the phenyl group.[53] The CP-OLEDs based on sky-blue enantiomers show a narrow emission and a high EQE_{max} of 32.1%. (*R*/*S*)-Czp-POAB) and (*R*/*S*)-Czp-terBuCzB show almost all mirror symmetric CPL signals in solutions, doped films, and devices. The g_{EL} factors in CP-OLEDs were +1.54 × 10^{-3} and −1.48 × 10^{-3}, +1.30 × 10^{-3} and −1.25 × 10^{-3}, respectively. This work demonstrates the incorporation of planar chirality into MR-TADF emitter as a reliable strategy for efficient CP-OLEDs.

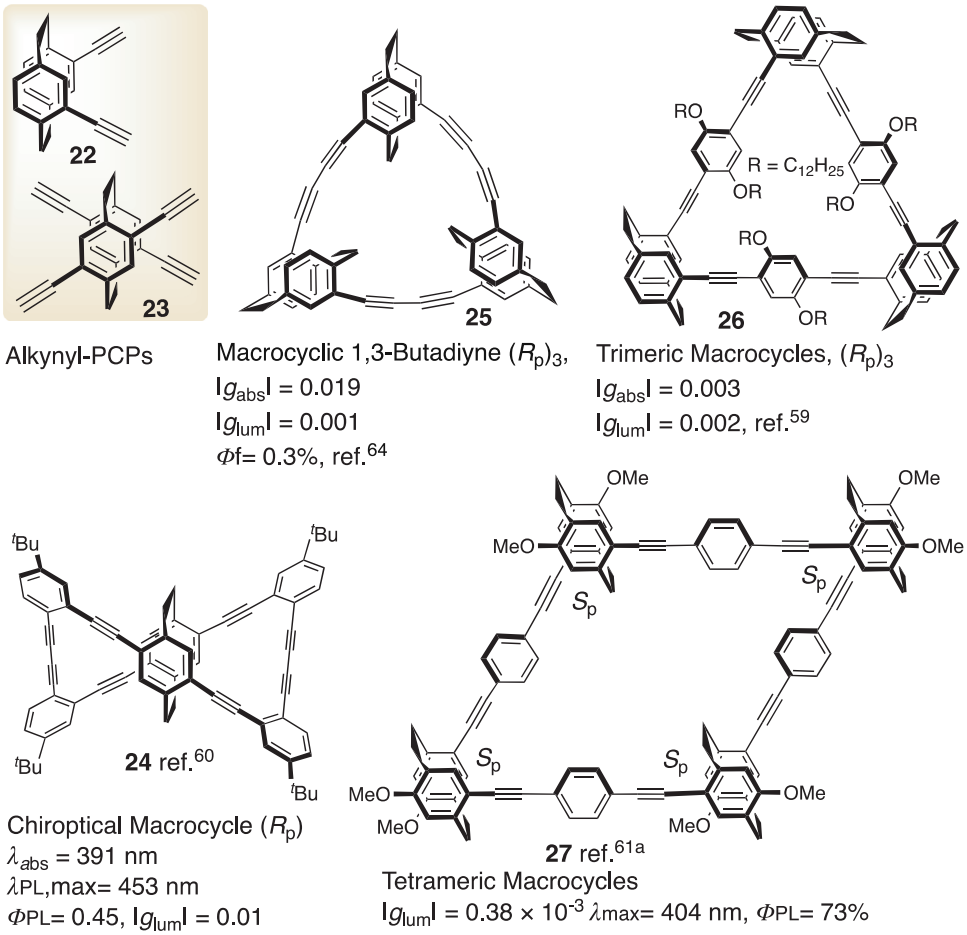

Figure 4. Ethynyl-PCP derivatives as precursors and PCP-based π-stacked through-space conjugated representative macrocycles.

Zheng and colleagues reported chiral room-temperature phosphorescent emitter that exhibit CPL properties with large g_{lum} of 7.2×10^{-3} and 1.2×10^{-2}.[54] During these investigations, CPL properties were modulated by incorporation of cyano(picolinonitrile) and 2,6-bis(trifluoromethyl)pyridine groups onto the carbazole-containing PCP enantiomers that extend the phosphorescence lifetime and longer afterglow. Through the elaboration of both decks of the PCP, that is, conjugation-extended carbazolophane donors (dicarbazolophane-based centrosymmetric core) decorated with triazine provided the solution-processed TADF compounds and EQE_{max} of 8.2% and an EQE of 7.9% at 100 cd m^{-2} was achieved.[55] The introduction of tert-butyl groups onto the triazine increases the solubility of targeted emitters in organic solvents, which is important for producing high-quality solution-processed devices.

3.2. Optically Active π-Stacked Macrocycles, Polymers, and Extended Structures Consisting of [2.2]Paracyclophanes

Pioneering research on PCP-based through-space conjugated molecules and polymers by Collard,[56] Morisaki and Chujo[57] employing electrochemical, metal-mediated cross-coupling, and various polycondensation approaches have opened up a new platform for the exploration of PCP-based materials in optoelectronic applications. This novel class of π-stacked polymers combines through-bond and through-space conjugation with the innate chirality of the PCPs into polymers with well-defined molecular weight that can act as single molecular wires. Morisaki and Chujo groups have introduced structurally-diverse π-stacked extended scaffolds with different geometries, sizes, and shapes including X-, V-, N-, M-, triangle-shaped, and helical structures exhibiting CPL activities. Ethynyl[2.2]paracyclophane derivatives as precursors (for instance **22** or **23**) can be connected via covalent bonds to synthesize PCP-based macrocycles (**24**), trimeric- (**25**, and **26**), and other tetrameric (**27**) macrocycles (**Figure 4**). These optically-active π-stacked extended molecules,[58] oligomers,[59] and macrocycles,[60] have been systematically investigated for tuning electronic and chiroptical properties.[61] Structurally-diverse and through-space conjugated poly(*p*-arylene-ethynylene)-type (PAE-type) π-stacked polymers built with varying bridge units (monomers) have been prepared with cyclophanyl cores. For instance, as illustrated in **Figure 5** polymer chain built with a PCP and incorporation of fluorene leads to an extension of the π-conjugation.[62] The polymers possessed good solubility in organic solvents, thermal stability and exhibited purplish-blue emission with high PL efficiencies in

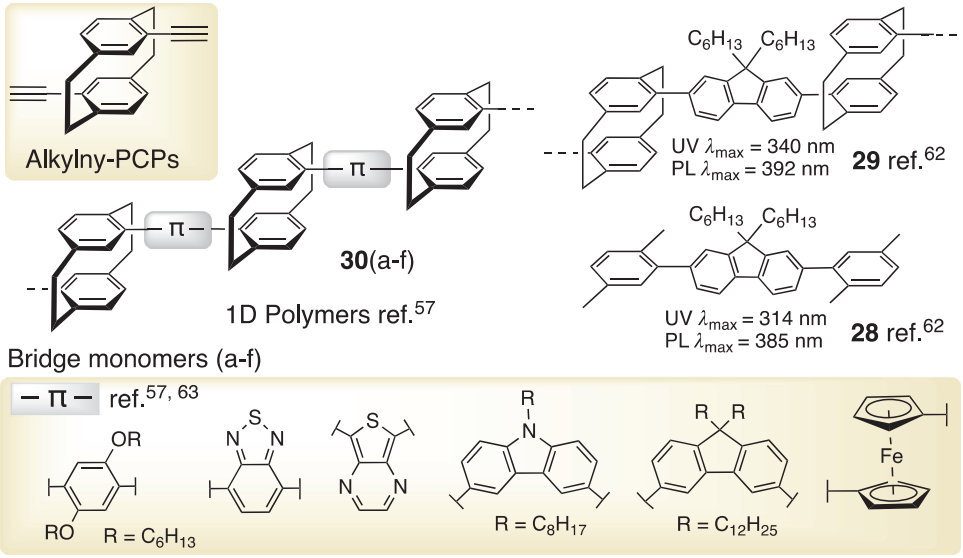

Figure 5. Through-space conjugated PCP-based polymers built with varying bridge units (monomers) and a reference compounds consisting of PCP with fluorene scaffold.

solution. The polymer **29** showed a strong absorption peak at λ_{max} of 340 nm, which was red-shifted relative to the model non-cyclophanyl compound **28** at λ_{max} of 314 nm. The fluorescence emission peak of polymer **29** observed at ≈392 nm in the visible purple-blue region with a high Φ_{PL} of 0.81. The emission of the model non-cyclophanyl compound **28** was slightly blue-shifted, while the absorption maximum of **28** exhibited a stronger blue shift of ≈25 nm. Different aromatic scaffolds can be incorporated into the polymers chains. The polymer characteristics can be controlled by appropriate tuning of the bandgaps and energy levels of the π-electron system. For in-depth synthetic discussions, details on theory, and optical and electrochemical properties of the PCP-based π-stacked polymers as models for semiconducting conjugated organic materials, readers are further referred to the focused book chapters.[63]

Mayor and colleagues have envisioned PCP-based π-stacked fully-conjugated all-carbon macrocyclic 1,3-butadiyne bearing three to six PCPs,[64] and other related macrocyclic oligothiophenes.[65] The heterocyclization of the macrocyclic 1,3-butadiyne bridges into macrocyclic 2,5-thienyls linked PCPs results into an increase in quantum yield and a significant redshift in emission wavelengths. Hasegawa have reported macrocyclic oligophenylenes, and biselenophene anchoring with stereogenic PCPs exhibited chiroptical properties due to the π-transannular interactions.[66] The resulting rigid biselenophene cyclic system exhibits enhanced chiroptical properties when compared with its acyclic precursor. Jiang and colleagues have introduced PCP-based nanosized chiral macrocycles with cycloparaphenylenes (CPP) backbone containing planar chiral pseudo *meta*-PCP (diethynyl-PCPs),[67] and 4,7,12,15-tetrasubstituted ethynyl-PCPs (referred to PCP-[n]CPP) for investigation on photophysical and chiroptical properties.[68] PCP-[6]CPP, PCP-[7]CPP, PCP-[8]CPP and PCP-[9]CPP were confirmed by single crystal X-rays analysis (the numbers in brackets are the number of benzene rings of CPP backbone). The macrocycles exhibit photophysical properties with high fluorescence quantum yield of up to 82%, and the fluorescence varies with the ring size from PCP-[6]CPP to PCP-[9]CPP. Size-dependent chiroptical properties with moderately large CPL dissymmetry factor (g_{lum}) of 1.9–2.9 × 10^{-3} and CPL brightness in the range of 30–40 M^{-1} cm^{-1} were observed. The CPL spectra of S_p- and R_p- are mirror images of each other. the (g_{lum}) values decrease with the increase of the number of benzene rings. Furthermore, in case of using 4,7,12,15-tetrasubstituted ethynyl-PCPs, the regioselectivity exerts a significant influence on the topological chirality was observed. The S_p-/R_p-PCP[12]-CPP were able to accommodate not only 18-Crown6, its complexes with protonated chiral amines in their cavity form a ring-in-ring complex and chiral ternary complexes along with excellent photophysical and chiroptical properties. In 2020, Duan and colleagues realized upconverted circularly polarized ultraviolet luminescence (UC-CPUVL) using PCP-based emitter built of chiral annihilator (*S*)−4,12-biphenyl[2.2]paracyclophane (R_p-, or its other enantiopure counterpart S_p-), and a TADF-sensitizer (carbazolyl dicyanobenezene, 4CzIPN).[69] R_p possessed a positive Cotton effect at 330 nm and a negative Cotton effect at 271 nm. Both enantiomers showed clear CPUVL emission at 380 nm, and its corresponding g_{lum} value was about 3.1 × 10^{-3}. R_p- and S_p- showed a mirror-image CD signals. After dispersing this upconversion system into room-temperature nematic liquid crystal, induced chiral nematic liquid crystal could significantly amplify the g_{lum} value (0.19) of UC-CPUVL emission that trigger enantioselective photopolymerization of diacetylene. This work provides a proof-of-concept for challenging chiral polymerization and paves the way for further development of functional application of CPL-active materials. There are other reports on exploring π-conjugated interactions by designing polymers with a mixture of π-face strapped and nonstrapped monomers.[70] Other discrete π-stacks, for instance, [2,2]fluorenophanes with excitonic coupling properties,[71] bisquinoidcyclophane as a candidate for multiphoton-gated optical materials (generated by the step-wise absorption of two photons from the corresponding tetraimidazoles),[72] *anti*-[2.2](1,4)anthracenophane, and

anti-[2.2](1,4)pentacenophanes with improved charge-transport materials properties have been investigated with the aim of tuning photophysical, optoelectronic, and electrochemical features of the systems.[73]

4. Supramolecular Polymerization Using Chiral [2.2]Paracyclophanes via Non-Covalent Strategies and Controlled Conformational Arrangements

Supramolecular polymers are defined as polymeric materials formed by reversible non-covalent interactions between functional monomers that result into polymeric properties in bulk and in solution.[74] Supramolecular polymerization rely on non-covalent strategies, for instance, π—π stacking, halogen bonding (X-bond), or better-known hydrogen bonds (H-bond), CH–π interactions and metal coordination to form diverse supramolecular systems with precise control over structure, properties and functions.[75] By bridging cyclophanes chemistry with supramolecular chemistry point toward new possibilities in cyclophane-based chiral materials applications.[76] Like most other prevalent arenes/heteroarenes systems, PCP scaffolds can be transformed by regioselective functionalization, and their chiral resolution provide PCP-based planar chiral 3D precursors capable of spontaneous organization into supramolecular assemblies. In this vein, exploiting non-covalent interactions of transannular (intramolecular) hydrogen bonds, Castellano and colleagues have demonstrated chemically-programmed 4,7,12,15-tetracarboxamide-substituted PCP as monomers (**31**) for spontaneous organization into well-define supramolecular polymer assembly with controlled conformational arrangements in solution and the solid state as depicted in **Figure 6**.[77] PCP are equipped with four hydrogen bonding units and the helical chiral sense of the assembly is dictated by the planar chirality (R_p or S_p) of the PCP monomers. Alkyl groups give solubility in organic solvents for solution studies. Upon assembly (e.g., of the R_p configuration), the planar chirality of the monomer is transferred to the helical-chirality of the supramolecular polymer. PCP stacks helically laced-up by two transannular H-bond strands made of PCPs though anti-aligned amides were confirmed by single-crystal X-ray analysis. An average intramolecular (transannular) H–bond (N···C═O) distance of 2.81 Å was revealed accompanying the well-optimized H-bonding distances of average amide torsion angles ($\varphi_1 \approx -38°$; $\varphi_2 \approx -141°$). While the average intramolecular distance between aryl ring centroids (3.1 Å) is fixed and consequently short, the intermolecular centroid-to-centroid distances are on-average larger 3.8 Å (the closest intermolecular $C_{aryl}\cdots C_{aryl}$ distance is 3.4 Å). NMR, IR, and UV–vis spectroscopic measurements have shown its persistence in organic solution. Supramolecular polymerization of the bridge-expanded homologue of PCP, namely, 5,8,14,17-tetracarboxamide-substituted [3.3]paracyclophane (**32**) which bearing an additional methylene unit -[CH_2]- in the [3.3]paracyclophane bridge, forms homochiral assemblies in nonpolar solution and the solid state through double-helical intermolecular and transannular hydrogen bonding.[78] The increased deck-to-deck π—π distance (3.3 Å versus 3.1 Å) due to the added bridge carbons, led to a change in the supramolecular structure of the assembly and results in a decrease in strain energy, and an increase in conformational freedom compared to the rigid PCP-based assemblies.

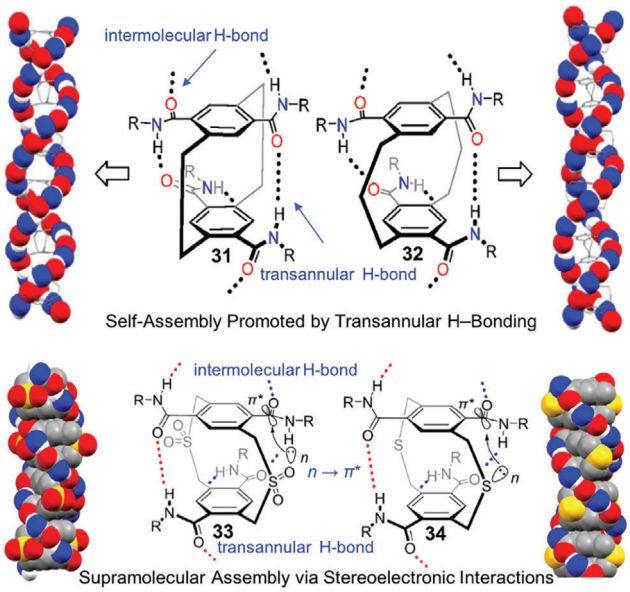

Figure 6. Supramolecular polymerization via non-covalent strategies of intermolecular and transannular H–bonding (top). Tuning supramolecular polymer assembly via stereoelectronic interactions employing [2.2]cyclophane versus [3.3]cyclophane and [3.3]thiacyclophane tetracarboxamides (bottom). Dashed lines indicate hydrogen bonding and $n \rightarrow \pi^*$ indicates stereoelectronic interactions. Reproduced with permission from ref. [77] Copyright 2016 Wiley-VCH; and from ref. [78,79] Copyright 2020 and 2021, American Chemical Society.

PCP substituted with four anilide (N-centered amide) hydrogen bonding units differ from amide hydrogen bonding units (C-centered/carboxamide versus N-centered/anilide, i.e., C_{ar}—C═O connectivity versus C_{ar}—N—C═O connectivity) influence molecular self-assembly with slightly longer H-bonds (average N···O distance 2.88 Å compared to 2.84 Å).

A new set of redox-tunable 2,11-dithia[3.3]paracyclophane tetracarboxamides differing in their bridge oxidation state (**33** and **34**) were investigated to understand the role of stereoelectronic interactions on tuning supramolecular polymer assembly (Figure 6; bottom).[79] An $n \rightarrow \pi^*$ interaction between the amide hydrogen bonding units and the central bridging atom results from the single-point exchange of the central methylene carbon atom for a sulfur atom (contacts between atoms with nonbonded electron pairs and carbonyls). This results in an increase in the elongation constant for dt[3.3]PCPTAS compared to that for their carbocyclophane analog [3.3]PCPTA. Changes in characteristic bond stretching frequencies, and geometric or structural changes of the supramolecular polymer assembly were evaluated by X-ray crystallography. All amides are participating in transannular and intermolecular self-complementary H-bonding. In the sulfide bridged dt[3.3]PCPTA-S, the bridging sulfur is engaged in a weak $n \rightarrow \pi^*$ interaction with the proximal amide carbonyls (d = 3.16–3.25 Å, θ = 82–102°). On oxidation of the sulfide to a sulfone (dt[3.3]PCPTA-SO_2, the sulfone oxygen engages the amide carbonyl in a stronger $n \rightarrow \pi^*$ interaction. Crystallographic evidence of a stronger n $\rightarrow \pi^*$ interaction is the elongation of the amide C═O bond. In the amides engaged in $n \rightarrow \pi^*$ interactions with the sulfone oxygen, the C═O bond is 0.011 Å longer than in

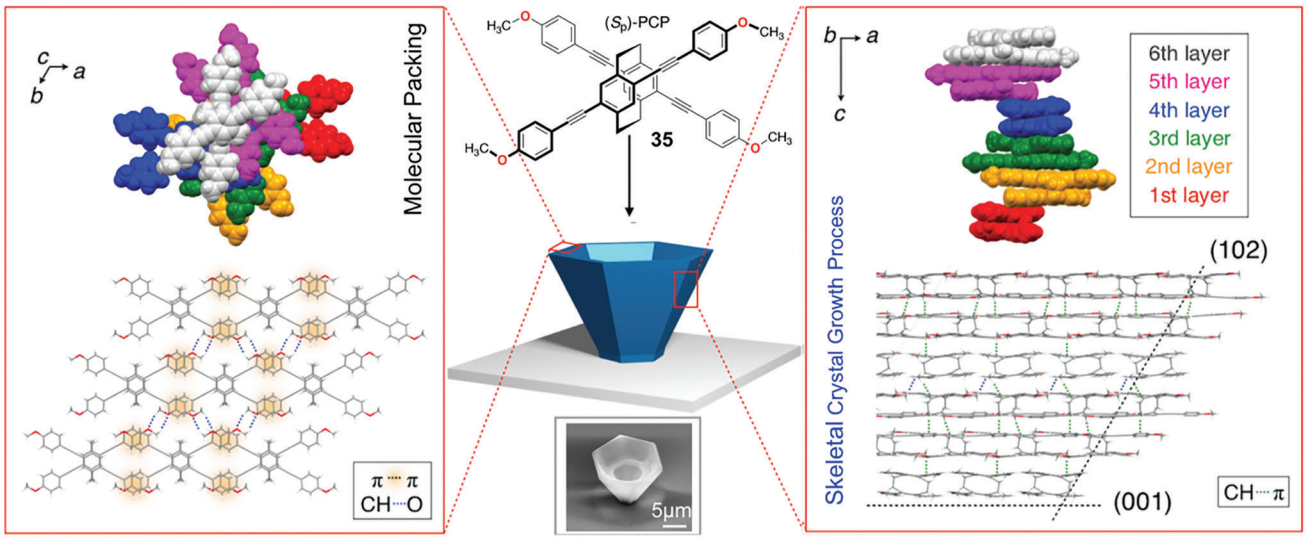

Figure 7. Morphological representation of the vessel-shaped skeletal chiral microcrystals; Molecular packing arrangement of the (S_p)-PCPs (bearing methoxyphenyl)ethynyl arms) in microvessel viewed from the c-axis (left) and b-axis (right) directions. The intermolecular interactions are visualized with orange circles (π—π), blue (C—H···O) and green (C—H···π) dashed lines. PCP molecules in each stack (layer) are colored red, orange, green, blue, magenta, and gray in order. SEM image of the microcrystalline vessel at scale bar: 5 μm. Reproduced with permission from ref. [80] Copyright 2022, *Science*, American Association for the Advancement of Science (AAAS).

those which are not engaged in $n \rightarrow \pi^*$ interactions (1.236 versus 1.247 Å). The molecular modeling of dt[3.3]PCPTAS revealed the potential for $n \rightarrow \pi^*$ interactions from the lone pair of the bridge sulfide sulfur or the bridge sulfone oxygen to the π^* orbital of the amide carbonyl. By oxidizing the sulfide to a sulfone bridge, this orbital donor–acceptor interaction can be strengthened which acts to shorten the donor···acceptor distance and increase orbital overlap. This acts as a secondary effect tuning the intermolecularly hydrogen bonded supramolecular polymer.

Exploiting non-covalent interactions, Oki and colleagues demonstrates an innovative synthesis strategy to craft crystalline chiral microvessels in a highly-controlled, hierarchically-organized uniaxial manner by stereoselective stacking of PCP-based chiral monomers employing drop-casting on various substrates.[80] The synchronous assembly of chiral skeletal single-crystalline microvessels emerges from the highly symmetric ordering of the chiral PCP monomers (**35**) that stack on one another via non-covalent interactions with a counter clockwise rotation of 60° along a crystallographic six-fold screw axis (**Figure 7**). The ingenious design of the PCPs appended with four (methoxyphenyl)ethynyl groups in enantiopure form brings the innate stereochemical features (planar chirality) and facilitates vital non-covalent supramolecular interactions which eventually lead to the stereocontrolled skeletal morphology. The solid-state structures investigated by X-ray diffraction on single crystals show multiple non-covalent forces of C—H···π, C—H···O and π—π interactions holding monomers together. Morphology control and transitions of the hierarchical crystal growth (from edge growth to facet growth) as well as thickness by stereoselective growth process were analyzed by scanning electron microscopy and in situ fluorescence microscopy observations. These microcrystalline vessels bear stereocontrolled skeletal morphology, recognize stereoisomers and serve as containers to accommodate microcrystals, polymer particles, and fluorescent dyes.

Functionalized PCPs bearing coordination-capable sites, for instance, carboxylic acid (COOH) have enormous potential to serve as organic ligands/linkers (**36–40**) and thus form supramolecular porous coordination polymers (also referred to as metal-organic frameworks MOFs). Appropriately functionalized organic molecules and inorganic metal nodes form porous coordination polymers via reversible coordination bonds, and find broad applications ranging from catalysis, sensing, separation, and porous carriers.[81] Organic building blocks bring structural/functional diversity into MOFs materials. Based on organic building blocks, metal type, oxidation states, and coordination capabilities, various geometries of coordination-driven reticular assemblies can be created for desired materials applications. PCP-derivatives are particularly appealing, inheriting the innate planar chirality and layered structure of the PCP once assembled into framework materials. PCPs functionalized with coordination-capable di- and tetratopic phenylcarboxylates in combination with $ZrCl_4$ to from crystalline zirconium-based 3D porous coordination polymers have been demonstrated (**Figure 8**).[82] This was the first demonstration where 9-connected Zr_6 nodes are incorporated in the framework using a PCP-linker, exhibit highly ordered periodic arrangements with rare net topologies. Using optically-active planar-chiral di- and tetratopic PCP-carboxylic acid form Zr-frameworks displaying strong CPL emissions exhibiting g_{lum} and Φ_{PL} values of up to 8.3×10^{-3} and 87% has been demonstrated which are amplified by ≈18- and 52-fold compared to the corresponding free PCP ligands.[83] This highlights the potential of optimizing CPL performances of chiral chromophores by using framework structures. PCP derivatives in combination with dipyridyl-substituted tetraphenylethene (TPE) motifs form non-covalent double

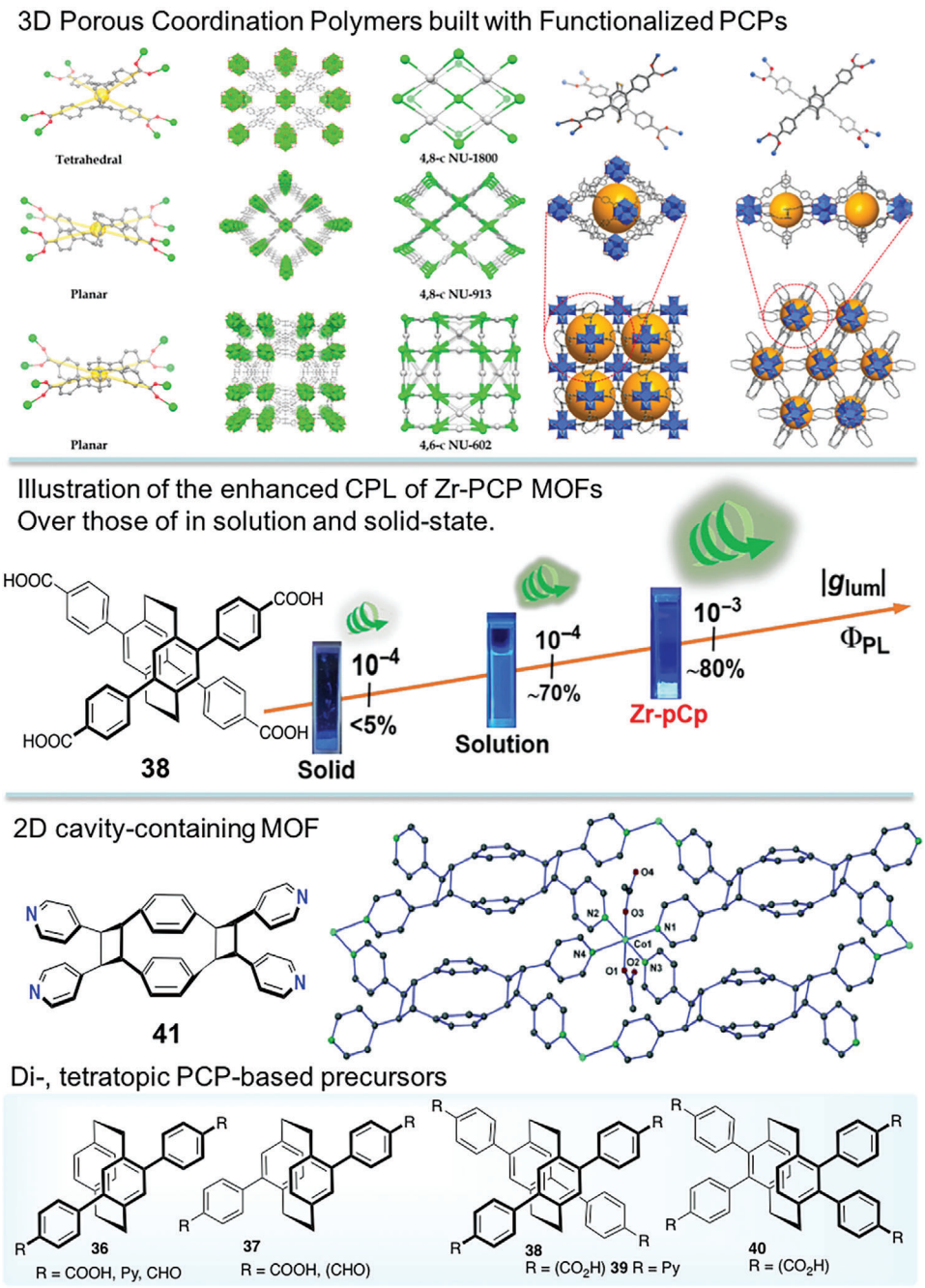

Figure 8. Supramolecular porous coordination polymers or MOFs constructed by coordination-driven strategies using di-, and tetratopic PCP-based precursors (top); Chiral Zr-PCP MOFs optimizing CPL performances of chiral chromophores (middle); 2D MOFs with multiple cavities built with tetrakis(4-pyridylcyclobutyl)-PCP in combination with Co(II) at the bottom. Reproduced with permission from ref. [82,83] Copyright 2022, American Chemical Society; from ref. [85] Copyright 2005 American Chemical Society.

helicates by metal-coordination which exhibit aggregation-induced emission (AIE) properties that could be useful for constructing artificial light-harvesting systems and CPL-OLED white LED devices.[84] TPE restricts the rotation of the phenyl rings and enables efficient chiral transfer from planar chiral PCP to the TPE fluorophore inducing efficient CPL.

MacGillivray and colleagues have demonstrated PCPs bearing multi-pyridyl end-groups, for example, tetrakis(4-pyridylcyclobutyl)-PCP (**41**) in combination with Co(II) nodes for constructing 2D supramolecular systems.[85] Other PCP-derivatives containing ditopic -COOH moieties directly attached at the pseudo- *para*- positions of the PCP,[86] and containing spacer-group of phenyl-COOH moieties at the *para*- positions of the PCP as well as bipyridines substituted PCPs to form coordination-driven supramolecular assemblies with various metal-precursors have also been demonstrated.[87] PCP-derived

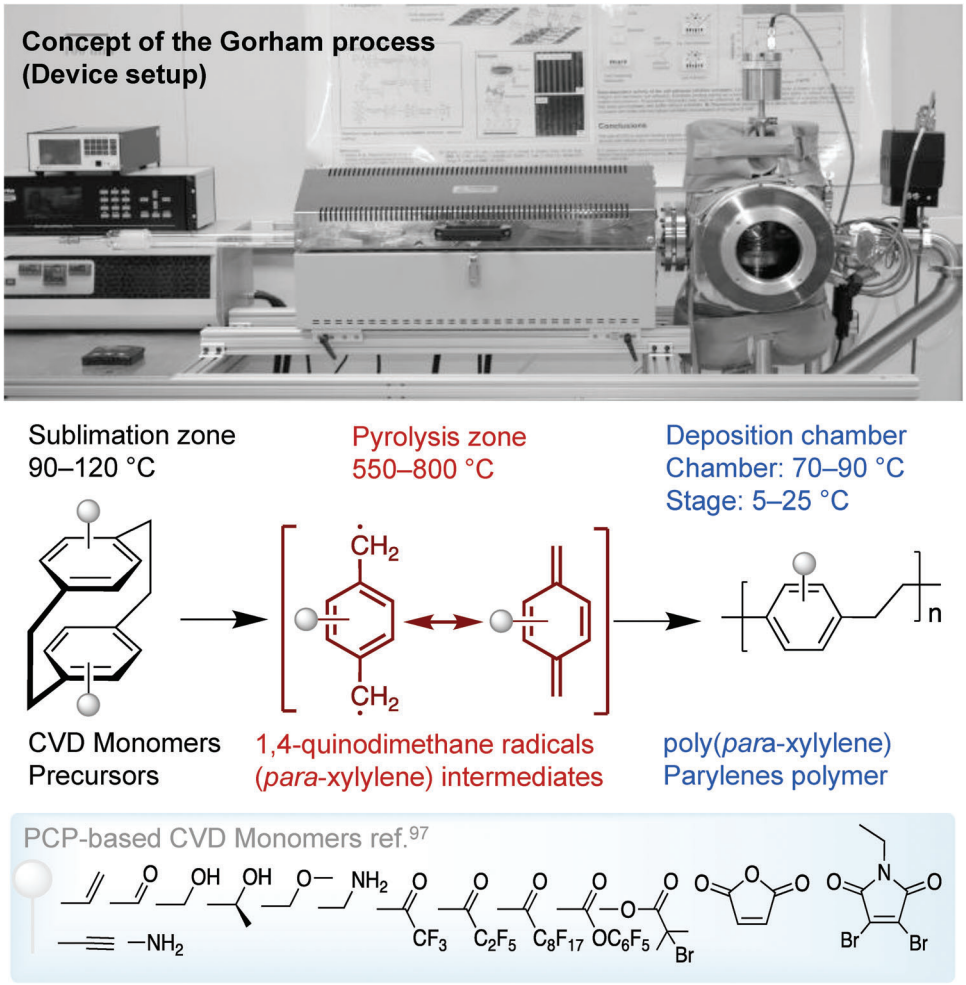

Figure 9. Concept of the Gorham process for PCP-based CVD polymerization (Parylenes) and library of CVD compatible functionalized PCPs as precursor monomers. Device diagram is courtesy of Lahann labs at KIT.

tetraldehyde in combinations with amine precursors to form crosslinked non-planar 2D covalent organic networks have been demonstrated.[88]

5. Cyclophane-Based CVD (co)Polymerization and Post-CVD Fabrication of Structurally-Controlled Parylene Polymer Surfaces

One of the main focuses of cyclophane research centers on polymeric poly(*p*-xylylene) coatings and their functionalized forms formed by chemical vapor deposition (CVD) polymerization using PCP-based precursors as gas-phase monomers (Gorham process).[89] The poly(*p*-xylylene) coatings are generally referred to their trade name parylenes. CVD polymerization is a widely used technology for making freestanding thin films or coatings on almost any surface where reactive species from chemical precursors are pre-formed in vapor phase and spontaneously polymerize into conformal homogeneous polymer surfaces. CVD polymers, because of their high purity, flexibility, and chemical inertness offer enormous potential of industrial importance ranging from microelectronics to photovoltaics, development of sensors, microelectrochemical materials, and have demonstrated technological utility as coatings of industrial products.[90] In contrast to the above described PCP-based layered-polymers prepared by cross-coupling, electrochemical, and various polycondensation approaches, however, the co-facially stacked layered-structure and planar chirality of the PCPs is lost during CVD polymerization process as the PCP core is cleaved homolytically at the ethylene bridges in a custom-built CVD device setup at high-temperature, and generates reactive intermediates of 1,4-quinodimethane radicals (*p*-xylylene) in vapor phase that spontaneously polymerize into homogeneous parylene polymer coatings. The general concept of the Gorham process of PCP-based CVD polymerization into poly(*p*-xylylene)s coating consists of sublimation, pyrolysis, and deposition and is depicted in **Figure 9**. A broad description of the fundamentals of poly(*p*-xylylene)s via cyclophane-based CVD polymerization methods, formation mechanism, structure controlling parameters and characterization techniques can be found in earlier reports.[91] For patterning on functional surfaces, techniques such as microcontact printing, photopatterning, using photomask or

lithographic techniques such as dip-pen nanolithography can be combined with CVD approach. CVD polymerization and its applications have been the subject of extensive research which are well-summarized in several recent focused-reviews, and book chapters.[92]

5.1. Design Strategies of PCP Precursors for Structuring Parylenes via Skeletal Composition and Post-CVD Fabrications

The chemical composition of a parylene polymer can be varied by altering the polymer backbone itself or by adding functional moieties as side-groups to tune their chemical, physical, and mechanical properties. For structuring parylene polymers and their functionalized forms (via skeletal modification) and their post-synthetic fabrications (via functionalization of the skeleton), the synthetic design of the chemically-programmed precursors, that is, CVD monomers is of fundamental relevance that determine its application sphere. For instance, commercial parylenes include parylene-N (**42**); the most common form is prepared from non-functionalized PCP.[93] Parylene-C (**43**) is prepared from mono-chloro-PCP, and parylene-D (**44**) is prepared from dichloro-PCP precursors. Parylene-HT or AF_4 formed from tetrafluoro-PCP (**45**), represent novel polymers with high thermal and chemical stabilities.[94]

Although, PCP components employed in CVD process are largely contain all-carbon backbones. By replacing one or both benzene rings with heteroaromatics, skeletally novel scaffolds consisting of two varying constituent units such as [2.2](2,5)pyridinophane, [2.2](2,5)pyrazinophane, *N*,*N*-dimethyl[2.2](2,5)pyrrolophane and pyridinophane derivatives (**46**) useful precursors for developing an entirely new class of functionalized polymers.[94] A diversity-oriented synthesis of perfluoro-PCP and brominated tetrafluoro-PCPs as CVD monomers has been developed.[28] PCP precursor bearing a stereogenic center as side-group, for instance, (S_p,*S*)−1-(4-[2.2]paracyclophanyl)ethanol and (S_p,*R*)−1-(4-[2.2]paracyclophanyl)ethanol (**47**) have also been prepared.

Modular synthesis approach in design and optimization of PCP as CVD monomers stands in the very center and remains a powerful route to parylene-derived functional materials. PCP-based precursors bearing synthetically tunable functional moieties, for instance, alkyne, thiol, hydroxyl, carbonyl, fluorinated groups, amino, ester, and anhydride components are compatible with the CVD polymerization conditions that can serve as anchoring sites for post-CVD surface engineering without alteration of the skeletal formats and brings ample opportunities and new capabilities.[95] Some of the PCP monomers used in CVD polymerization and post-CVD fabrication of reactive poly(*p*-xylylene)s are described in **Figure 10**. Molecular systems do not have to be limited to the mentioned few examples of PCPs. There are diverse other structures that share similar structural and functional features, which have been well-optimized for CVD process.

5.2. Structuring Multi-Functional Parylene Surfaces via CVD Copolymerization and Post-CVD Fabrication Strategies

Chemical modification of poly(*p*-xylylene)s surface by specific functional moieties allows tuning surface properties through post-CVD fabrication while preserving the inherent polymer backbone.[96] For post-CVD fabrication process via covalent binding, employing chemical methods of azide–alkyne "click" chemistry, light-induced thiol–ene/thiol–yne reactions, aldehydes/ketones with hydrazides or alkoxyamines, and other approaches have been developed for surface tailoring via post-synthetic fabrications.[97] Lahann, Chen, and colleagues in their independent reports have reviewed the most recent advances in PCP-based CVD polymerization and post-CVD fabrication that provide a comprehensive overview from the overall application perspectives particularly for biointerfaces engineering.[98]

By employing multiple PCP monomers, each substituted with a functional moiety of different chemical reactivity, enable CVD copolymerization to form multi-functional reactive polymeric parylene surfaces with anchoring sites that can be further fabricated in post-deposition surface engineering. For instance, a two components copolymerization in a custom-built CVD device setup by employing 4-*N*-maleimidomethyl-PCP and 4-methyl-propiolate-PCP components generates poly[(4-*N*-maleimidomethyl-*p*-xylylene)-*co*-(4-methyl-propiolate-*p*-xylylene)-*co*-(*p*-xylylene)] functional polymer.[99a] Using 4-*N*-maleimidomethyl-PCP and 4-methyl-propiolate-PCP components in CVD copolymerization generates multicomponent coating of poly[(4-*N*-maleimidomethyl-*p*-xylylene)-*co*-(4-methyl-propiolate-*p*-xylylene)-*co*-(*p*-xylylene)]. Methyl propiolate and maleimide attached to the CVD polymer enable biorthogonal click reactions with azide-terminated biomolecules, and Michael-type thiol coupling reactions with maleimides (**Figure 11**).[99b] This approach has been adopted for structuring various multifunctional parylene surfaces.[100]

In a similar way, the concept of a three component CVD copolymerization generates polymer surfaces with trifunctional moieties. For instance, acetylene, maleimide, and ketone (by employing three different precursors of 4-ethynyl-PCP, 4-*N*-maleimidomethyl-PCP, and trifluoroacetyl-PCP) has been demonstrated.[101] Trifunctional polymer surfaces could enable specific functions via conjugation of Alexa Fluor-555 azide, fluorescein-labeled cysteine, and Alexa Fluor-350 hydrazide, respectively, as model reporter molecules (**Figure 12**). This concept is well-optimized to control the immobilization of biomolecules selectively under mild conditions similar to biological environments, their broad translational potential yet to be developed.

In a rather different strategy of CVD copolymerization using a PCP component in combination with a non-cyclophanyl component of cyclic ketene acetal (namely; 5,6-benzo-2-methylene-1,3-dioxepane) forming polymer backbone bearing degradable ester-linkages has also been developed.[102] The degradation kinetics were dependent on the ratio of the PCP to the ketene acetal precursor. This concept combines interfacial multifunctionality with hydrolytic degradability in CVD polymers, opening up new application possibilities.

Beyond the conventional trends, dimensionally-organized structuring of parylenes could bring new capabilities and opportunities in CVD polymerization. Integrating CVD polymerization process with a template-driven fabrication techniques enable to achieve topologically-defined structuring of parylenes (in 1D to 3D dimensions) with tailored shapes, sizes, and chemistries. To demonstrate the spatially organized thin-films fabricated by CVD, Lahann and co-workers have investigated liquid crystals

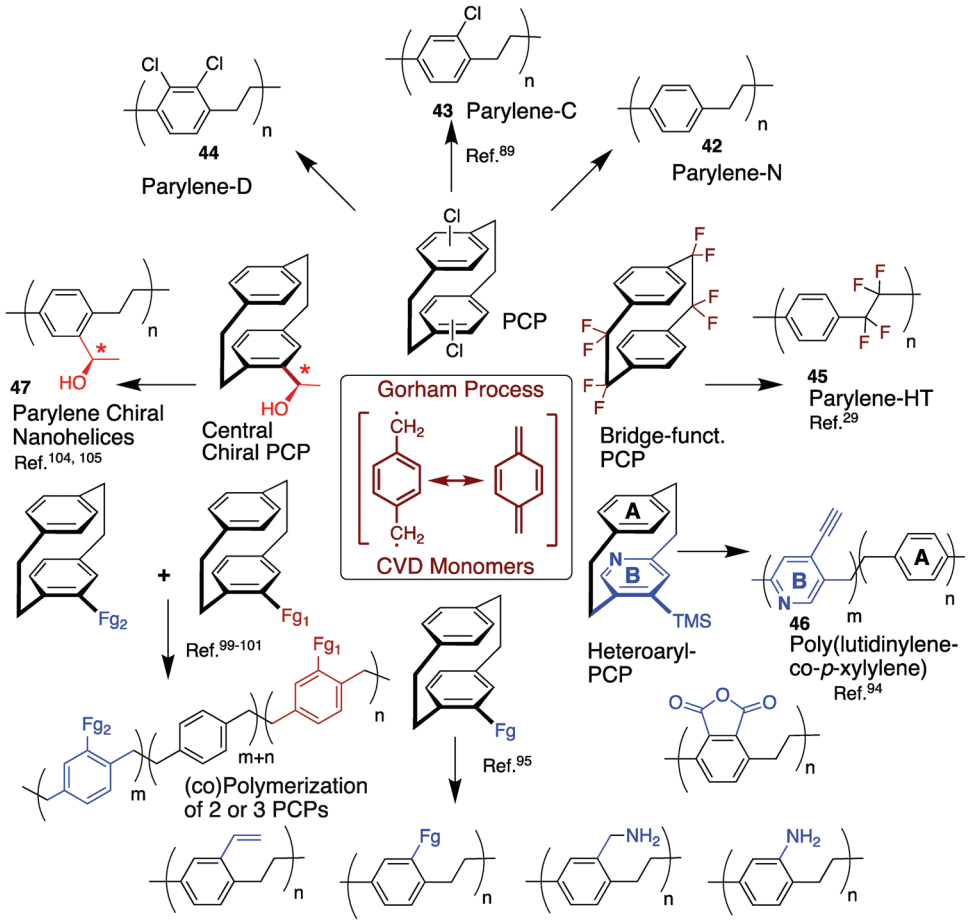

Figure 10. Generalized structural and functional design of the reactive poly(*p*-xylylene) coating/surfaces by CVD (co)polymerization.

(LCs) as template for CVD polymerization to prepare nanohelices of parylene polymers on surfaces with tunable length, pitch, and higher-order mesoscale morphologies by varying the chirality of the template.[103] Straight fibers were obtained by using nematic LCs, while nanostructures with pores of ≈500 nm in diameter were yielded by using blue-phase LCs (**Figure 13**). By using cholesteric LCs, the helicity could be transferred to the nanofibers in the form of a spiraling of the fiber in the μm range. Upon removal of the LCs template, the morphology and structural regularity of the template remain preserved.

As mentioned earlier, the co-facially stacked 3D structure and stereochemical features (element of the planar chirality) of the chiral PCPs cannot sustain during CVD polymerization process at high-temperature. However, by incorporating an additional stereogenic center (for instance, by adding central chirality) in the side-group attached to the PCP precursors can transcript conformational features of the monomers into the corresponding CVD-based polymeric materials. PCP precursor bearing a stereogenic center as side-group (**47**), for instance, (S_p,*S*)−1-(4-[2.2]paracyclophanyl)ethanol and (S_p,*R*)−1-(4-[2.2]paracyclophanyl)ethanol enable the formation of chirality-defined superhierarchical arrays of nanohelices via CVD polymerization into supported films of LCs (**Figure 14**).[104] The CVD fiber reflects twists (*S* or *R*) depending on the PCP-monomer handedness, and this opposite helicity shows a mirrored signal in the CD spectrum. In contrast, templated CVD polymerization of the achiral PCP precursor under identical conditions resulted in straight nanofibers rather than nanohelices. These findings outline a new approach toward polymer nanostructures, as morphological design features can be templated aiming for 3D soft-matter architectures. The chiral information is directly encoded into the PCP precursors rather than the templating LCs medium. Using carefully chosen reaction parameters and synthesis routes: that is, i) regioselective functionalization of the PCP, ii) followed by chiral resolution step, and iii) successive transformations afford optically active planar and central chiral PCP precursors in an enantioenriched form.[105]

The CVD polymerization of chiral PCP precursor ranging from 0% e.e. to 100% e.e. of the *S*-configured precursor was studied. SEM revealed that the morphology of the resulting nanofibers prepared with different % e.e. of chiral precursor was markedly different. With 0% e.e. chiral precursor, the resulting nanofibers were mostly un-twisted. Strong bisignate CD signals were found for twisted nanofibers at 247 nm. It is hypothesized that as the molecular size of the chiral center increases, the degree of the steric effect should increase and thus the degree of twisting should increase as well. Demirel and colleagues have reported poly(*p*-xylylene) containing free-standing,

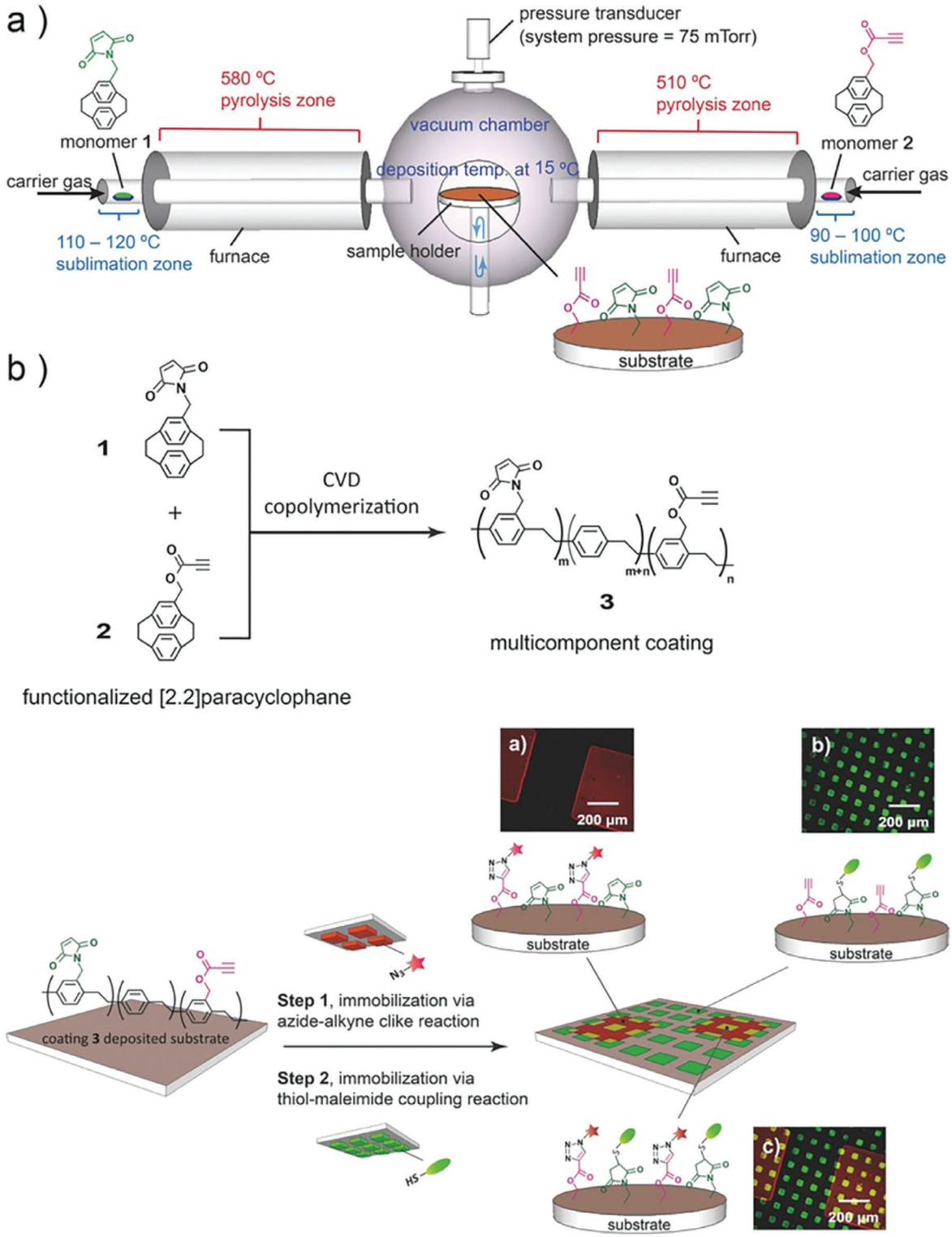

Figure 11. Top: a) Schematic illustration of a two-sourced CVD copolymerization used to prepare the multicomponent coating. b) CVD copolymerization of a 1:1 molar ratio of 4-(*N*-maleimidomethyl)-PCP (**1**) and 4-methyl-propiolate-PCP (**2**) to form poly[(4-*N*-maleimidomethyl-*p*-xylylene)-*co*-(4-methyl-propiolate-*p*-xylylene)-*co*-(*p*-xylylene)] (**3**). Bottom: Schematic illustration of multicomponent coating and immobilization of multiple biomolecules by biorthogonal approach. An azide–alkyne click immobilized the Alexa Fluor-555 azides, and a thiol–maleimide coupling was used to immobilize fluorescein-labeled cysteines. The process of µCP was used to confine specific conjugation to selected areas. a) The red-channeled fluorescence microscopy image illustrates the immobilization of the Alexa Fluor-555 azides. b) The green-channeled fluorescence microscopy image reveals the immobilization of the fluorescein-cysteines. c) Overlaid images of (a) and (b). Schemes and images are reproduced from ref. [99b] Copyright 2014, Wiley-VCH.

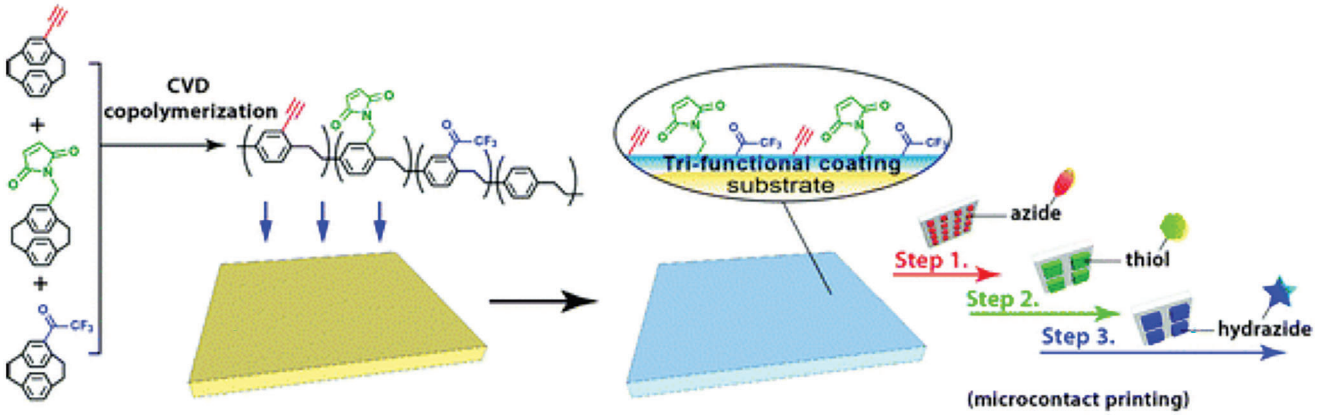

Figure 12. a) Representation of three component CVD copolymerization and tri-functional coating homogeneously deposited and subsequent immobilization molecules of Alexa Fluor-555 azides (red), fluorescein-labeled cysteines (green), and Alexa Fluor 350 hydrazides (blue). Schemes and images are reproduced from ref. [101] Copyright 2013 Royal Society of Chemistry.

slanted, parallel columns.[106] Recently, using a 3D porous template of metal-organic framework crystals for poly(*p*-xylylene)s via CVD polymerization with implementation of 3D spatial arrangements establishes a new platform for the synthesis of functional parylene polymer particles with structurally controlled morphologies, where molecularly imprinted structuring can be modulated by the choice of both the template and the CVD precursors.[107] To exploit this approach, a large diversity of crystalline porous-framework materials is available with variable crystal sizes, shapes, and pores that can serve as confined templates for the synthesis of 3D polymer nanostructures, as has been demonstrated successfully in liquid-phase polymerization.[108] Chen and colleagues have envisioned a multifunctional CVD copolymerization on sublimating ice particles as template at the dynamic vapor–solid interface to fabricate a porous and multifunctional poly-*p*-xylylene material.[109] The vapor-phase sublimation and deposition occurs simultaneously, where the deposition of the poly(*p*-xylylene)s occupies the space vacated by the subliming ice (**Figure 15**).

Poly(*p*-xylylene)s surfaces containing ester alkyne and maleimide functionalities were used to demonstrate the concept of multifunctional porous poly(*p*-xylylene)s by immobilizing

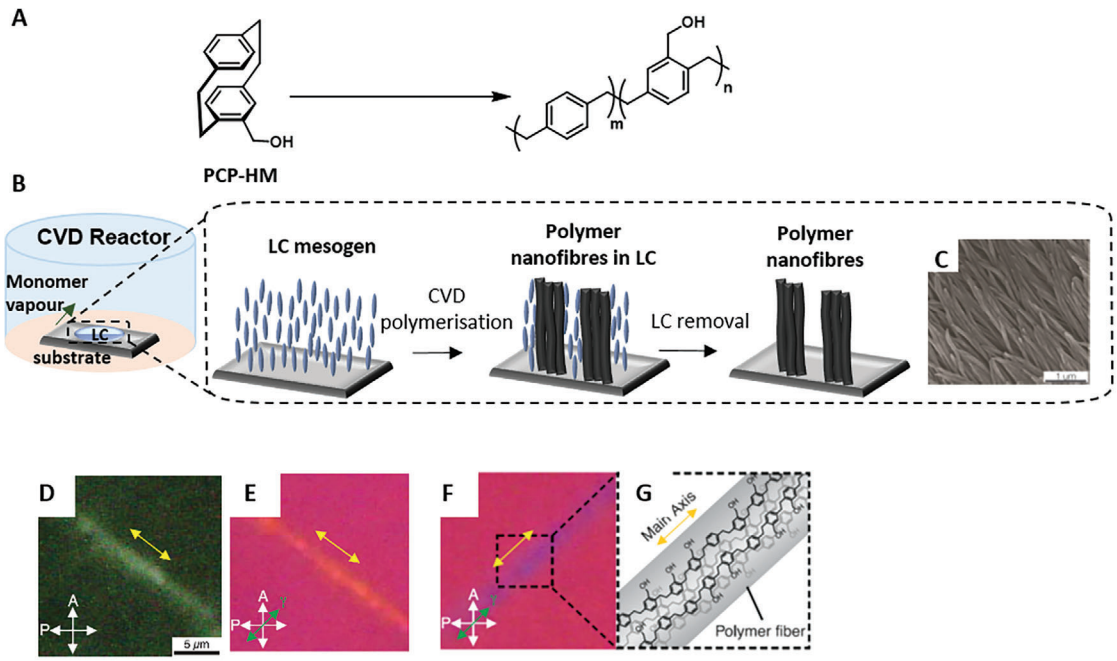

Figure 13. Templated synthesis of polymeric nanofibres using surface-anchored LC phases as templates. A) CVD of 4-hydroxymethyl-PCP to yield the respective polymer; B) Fabrication of polymer nanofibres via CVD into homeotropically aligned LCs; C) Scanning electron microscopy (SEM) image of nanofibres after LC removal; D) Optical micrograph (cross polarisers) of a nanofiber, where A and P are the orientations of the polarisers; E, F) Micrographs of a nanofiber with a quarter-wave plate with its slow axis; G) Alignment of the polymer chains along the axis of the fiber. Reproduced with permission from ref. [103] Copyright 2018 *Science*, American Association for the Advancement of Science (AAAS).

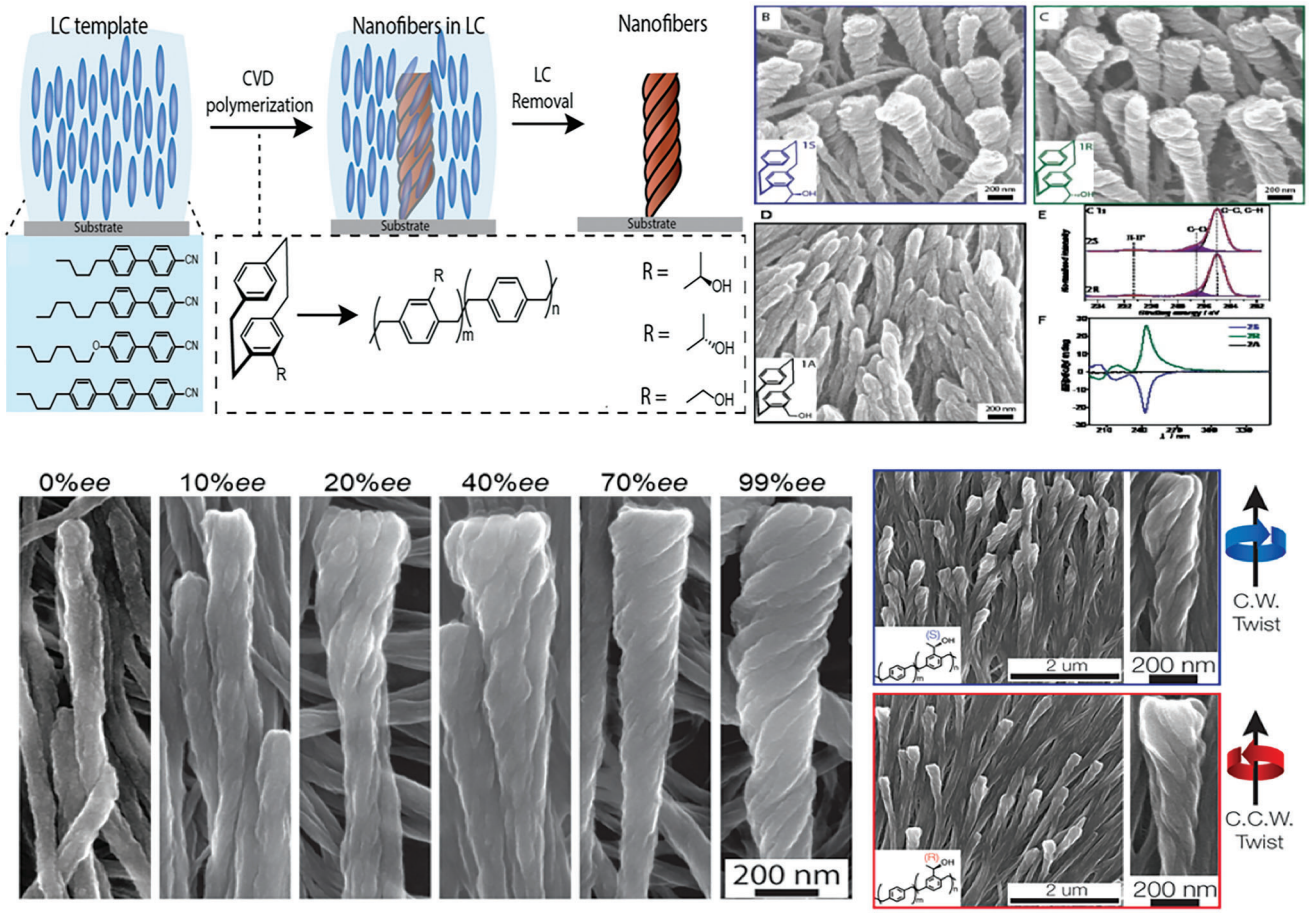

Figure 14. Template-driven synthesis of polymer nanohelices via PCP-based (**47**) CVD polymerization into a nematic LC film. A) Top; Templated synthesis of polymer nanohelices via CVD polymerization into a nematic LC film. Inset: Chemical representation of CVD polymerization of chiral and achiral precursors. B–D) SEM images of nanohelices *S* and *R* and achiral nanofibers A prepared by CVD polymerization of 1*S* (B), 1*R* (C), and 1A (D), respectively (the LC is homeotropically anchored on a surface before polymerization and was removed prior to SEM). E) High-resolution C1s XPS spectra of *S* and *R* confirming identical chemical composition for nanohelices with opposite handedness; these spectra are identical to the achiral nanofibers. F) Circular dichroism spectra of nanohelices *S* (blue) and *R* (green) and achiral nanofibers A (black). Bottom; Influence of enantiomeric excess on fiber helicity shown as SEM images. SEM images of the nanofibers and the induced mesoscale chirality of (+)-(S_p,*S*) and (+)-(S_p,*R*)-PCP with varying % enantiomeric excess upon polymerization into nematic E7. (blue) *S*-configured or (red) *R*-configured into a thin film of LC (MDA-98-1602). LC was removed prior to imaging. Reproduced with permission from ref. [104a] Copyright 2021, Wiley-VCH.

the fluorescence probes, Alexa Fluor 555-labeled azide, and fluorescein-labeled (FITC) cysteine. Huisgen 1,3-dipolar cycloaddition to click azides and terminal alkynes, and the maleimide moiety provides an efficient pathway toward the conjugation of a thiol group via Michael-type addition with the formation of a stable thioester bond. Templated CVD opens a new platform for designing PPX with programmable geometry, alignment, and chemistry.

6. Cyclophanediene Precursors Design Strategies and Poly(*p*-phenylenevinylene) Polymers by Ring-Opening Metathesis Polymerization

Cyclophanediene and related strained cyclophanes have emerged as useful precursors for ring-opening metathesis polymerization to prepare poly(*p*-phenylenevinylene)s (PPV)s conjugated polymers for electronic and optical applications.[110] PPVs, a class of the conductive polymers consist of alternating alkene and phenyl groups in conjugation.[111] [2.2]Paracyclophane-1,9-diene (**49**) has gained attention as a monomer in PPVs (via ROMP) obtained with *cis*/*trans* configuration which could be isomerized to the all-*trans* polymers upon photochemical stimulation as documented in literature.[112] The development of functional-group tolerant and robust olefin-metathesis catalysts has enabled the use of diverse cyclophane monomers in ROMP, with the possibility of block (co)polymerization and end-group modification due to its living nature.[113] In 2006, Turner and colleagues reported pioneering research describing the polymerization of tetraoctyloxy-[2.2]paracyclophane-1,9-diene by ROMP to prepare soluble poly(dioctyloxy-*p*-phenylenevinylene).[114] This approach has been investigated for over a decade, amongst others, by Turner and colleagues have intensively studied the chemical reactivity of various catalysts-types (**50–53**), monomer-to-catalyst ratio in combination with varying PCP-ds featuring different

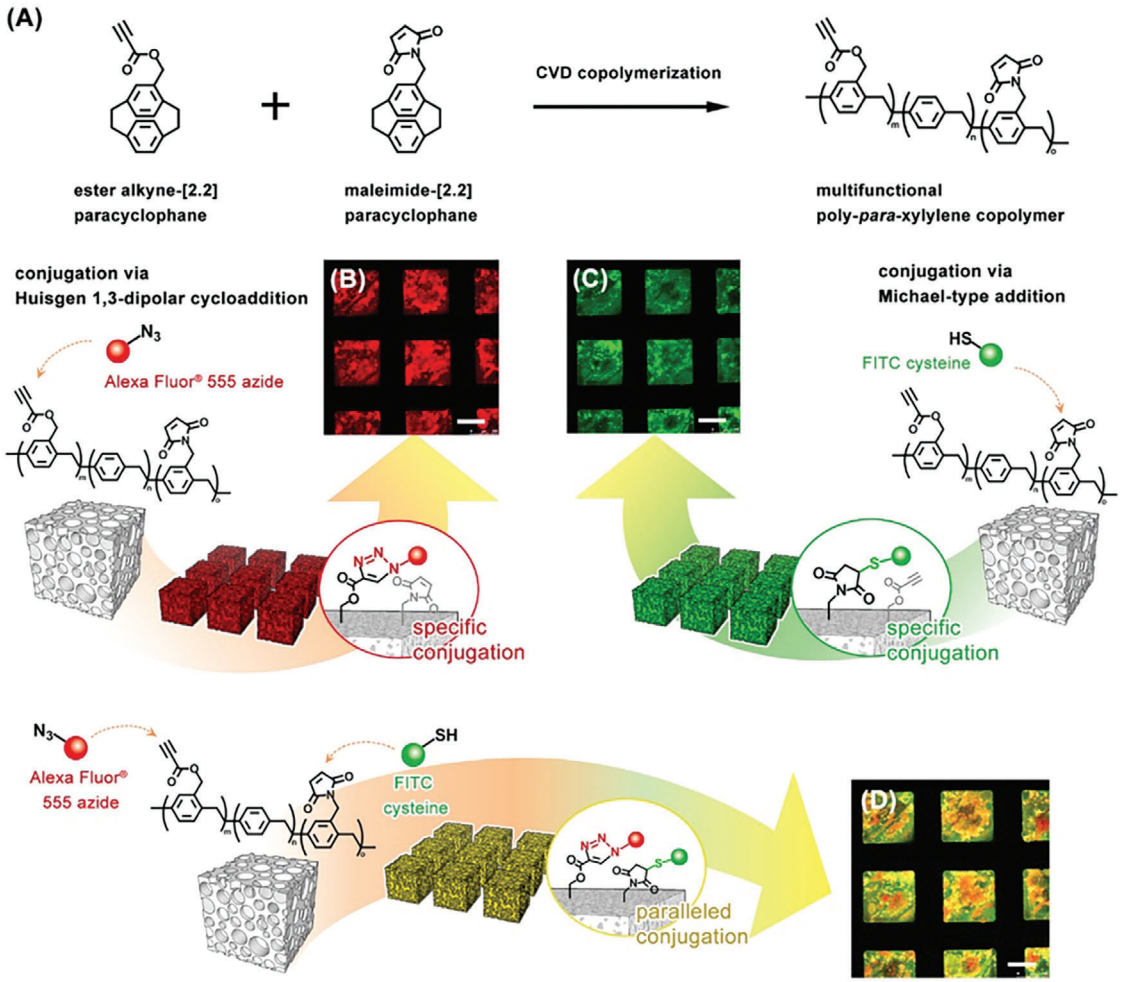

Figure 15. Multifunctional CVD on ice template: A) Reaction scheme using ester alkyne- and maleimide-functionalized *p*-xylylenes for copolymerization and deposition on the same ice template substrate to fabricate a porous and multifunctional poly-*p*-xylylene material; B) Fluorescence micrograph showing the specific conjugation of Alexa Fluor 555-azide (red channel) toward the ester alkyne groups on the interface of the porous material; C) Fluorescence micrograph showing a second and specific conjugation of FITC cysteine (green channel) toward the maleimide groups on the same porous material; D) Paralleled conjugations of the two fluorescence molecules (overlaid image). Scale bars: 250 µm. Reproduced with permission from ref. [109a] Copyright 2020, American Chemical Society.

regiochemistry and substitutes attached to the (hetero)aromatic core for modulating soluble PPVs (**Scheme 2**).[115] The driving force for ring-opening and polymerization is strain relief. Attaching alkyle or alkoxy side-chains to the PPV polymer backbone increase solubility. In ROMP the chemical nature of the PCP-d substituents on the monomer also have an influence on the kinetics of the reaction. Choi and Zentel's investigated the reactivity behavior and the polymerization process of four isomeric alkoxy-substituted PCP-ds (e.g., **57**) in combination with several catalysts in ROMP.[116] ^{1}HNMR spectroscopy was used for monitoring the initiation process via the carbene signals. The chemical shifts of the initiated species vary depending on the NHC ligand and the coordination of the aryl-ether (2-ethylhexyloxy or methoxy). The coordination of the monomer repeating unit to the Ru-catalyst during the polymerization process was envisioned. It was revealed that the introduction of aromatic ethers should be applied especially to monomers of low reactivity to obtain a long-living catalyst species with increased stability and enable polymerization even under harsh conditions of high temperatures are needed. A detailed investigation of the ROMP of alkyl- and alkoxy-substituted PCP-ds were carried out by Turner and colleagues. Complexation of the ruthenium center by the oxygen of the alkoxy substituent was observed in ^{1}HNMR and ^{13}PNMR spectroscopy of the reaction and leads to significantly slower rates of propagation than those observed for the alkyl derivative. The effects of differing arene size on the structure, strain energy, and chemical reactivity of the cyclophanediene have been examined by Weck and colleagues.[117] Conjugated block copolymers can be prepared by sequential monomer additions. Elacqua and colleagues have introduced programming donor-acceptor sequence-defined ROMP approach by using unsymmetrical PCP-ds.[118] By incorporating an electron-rich dialkoxyphenylene and electron-deficient benzothiadiazole rings within the PCP-d monomers (**58** and **59**) represents an ideal platform to investigate the combined impact of steric and electronic effects, thus ROMP using ruthenium carbene initiators give donor-acceptor

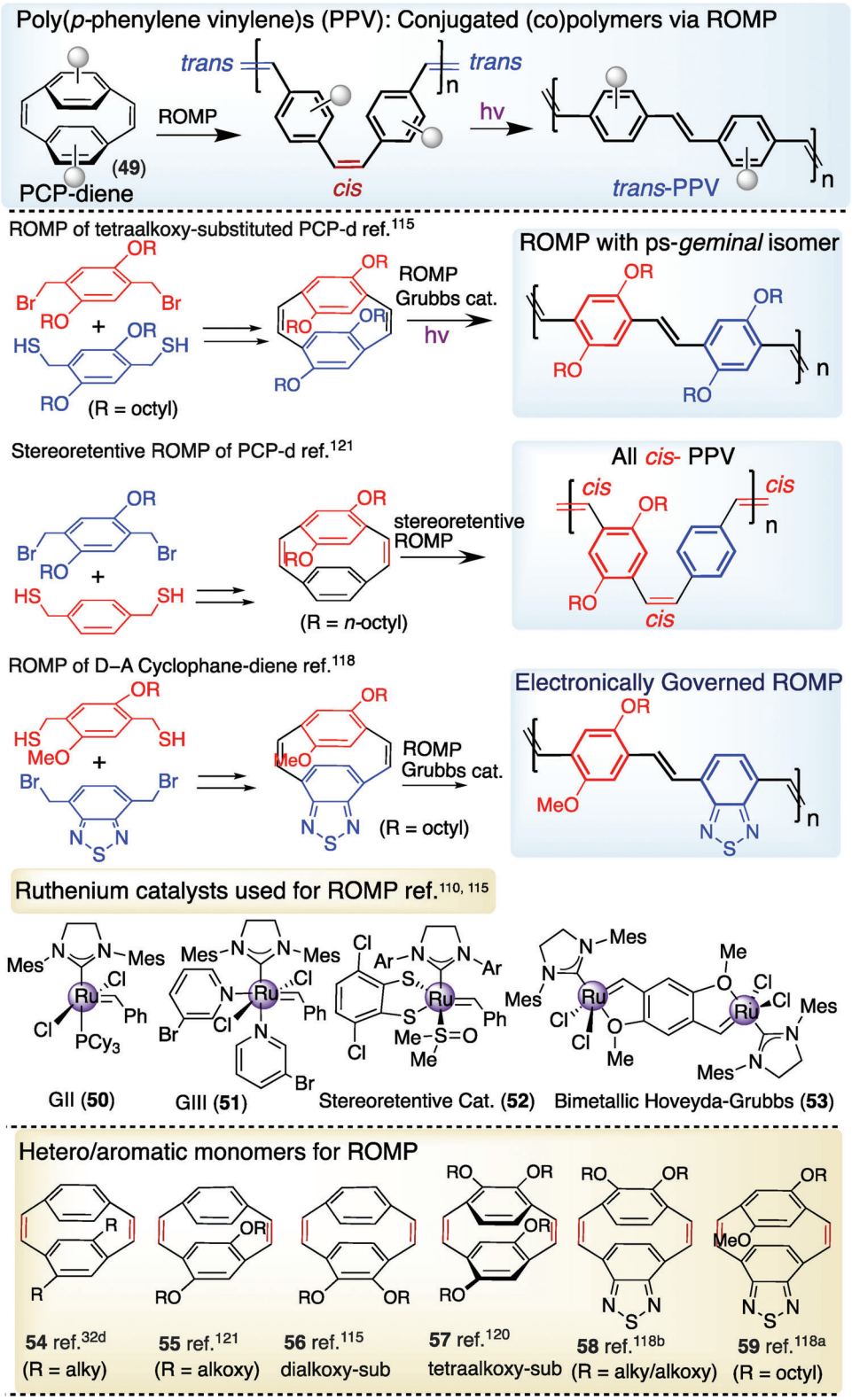

Scheme 2. General synthetic routes toward some PCP-d derivatives and the concept of ROMP using PCP-d and its photoisomerization into all-*trans* PPV polymer.

alternating poly(*p*-phenylenevinylene) benzothiadiazole copolymers that can be photoisomerized in dilute solution to the corresponding all-*trans* derivatives.[119] The donor–acceptor polymers were well-defined ($Đ = 1.2$, $M_n > 20$ k) and exhibited lower energy excitation and emission in comparison to polymers formed from other processes.

ROMP generates (co)polymers featuring alternating *cis*/*trans*-poly(*p*-phenylenevinylene)s.[120] Michaudel and colleagues have recently introduced the synthesis of stereo-defined all-*cis* poly(*p*-phenylene vinylene)s with living characteristics and exquisite control over the polymer chain growth via stereoretentive ROMP approach using PCP-d bearing either a linear alkyl or a branched alkoxy substituent.[121] The level of control enabled by stereoretentive dithiolate-chelated Ru-based catalysts (**52**) (first prepared by Hoveyda and colleagues)[122] provides a new platform for synthesizing PPVs with excellent solubility in organic solvents (including THF, C_6D_6, CH_2Cl_2, and $CDCl_3$). The phototunable nature that can be isomerized with UV light, could possibly allow the synthesis of all-*cis* PPVs embedded in complex polymeric architectures might find broad applications as stimuli-responsive materials.

Weck and colleagues have envisioned living/iterative ROMP containing terminal recognition sites for hydrogen bonding or metal-driven coordination to fabricate supramolecular block copolymers that can mimic covalent rod–coil–rod architectures featuring orthogonal stacking. The directional self-assembly approach enables the achievement of semiconducting block copolymers and can combat conjugated polymer aggregation.[123] Azide-functionalized PPVs enables to incorporate any desired moiety to PPV in post-polymerization modifications through alkyne–azide click reaction which is a commonly employed strategy that has already been reported for PPVs synthesized by non-living methods.[124] This strategy represents a key advance in materials for potential applications.

There are of course other important research contributions made in cyclophane chemistry that are quite relevant to the particular theme of this report. Herein some pioneering research in cyclophane chemistry is highlighted and representative articles are enlisted. My apologies! if any studies in cyclophanes chemistry might be unintentionally overlooked. All such efforts to the progress of this field are greatly acknowledged.

7. Summary and Outlook

One of the most fundamental and principal aspects of [2.2]paracyclophane chemistry will remain the development of planar chiral ligand and catalyst systems as useful toolbox for stereo-controlled synthesis. With ever-growing numbers of diverse chiral ligands and catalysts being reported, exploring new concepts, and designing strategies based on planar chirality as a viable alternative to the most conventional central/point chirality offer the opportunity for improvements to further progress. For chemists who are pleased by manipulation of symmetry properties, the cyclophanes provide an art form. Cram in his famous article entitled "Cyclophane Chemistry — Bent and Battered Benzene Rings" published in *Accounts of Chemical Research* in 1971 concludes with the following: "The chemistry of the PCP will be completed only when chemists tire of tinkering with them" (D. J. Cram, J. M. Cram, *Acc. Chem. Res.* **1971**, *4*, 204). After almost 75 years since the discovery of PCP "Preparation and Structure of Di-*p*-Xylylene," experimental and theoretical efforts still continue to establish how and why *para*-quinonedimethide is converted into [2.2]paracyclophane and polymeric parylene (di-*p*-xylylene) as recently reported by Sherburn, Coote, and colleagues on "Computational and Experimental Confirmation of the Diradical Character of *para*-Quinonedimethide" *J. Am. Chem. Soc.* **2023**, *145*, 16037.[125] After 75 years of research and developments, it still holds many surprises due to unusual chemical reactivity. Even in certain cases the results may not be predictable under the established classic reaction conditions.

We have learned in the course of our journey in cyclophane chemistry that synthesizing some specific PCPs for a particular purpose to show their useful utility in materials fabrication can be a tedious endeavor because regioselective functionalization and resolution strategies pose certain synthetic challenges due to the unusual reactivity of PCP, especially when larger quantities of enantiomerically pure PCPs are needed which is often viewed as limiting steps in expanding this class of monomers/precursors for materials fabrication. Hence, developing efficient synthesis methods for selective derivatization of the PCPs, and their resolution would contribute to further progress in this field.

PCPs chemistry combines traditions of classics with innovations to enable new functions. Chemists collaborate with experts from other areas of chemical science and materials engineering. In this spirit, capitalizing on collaborative research efforts within the chemistry community and ensuing holistic approaches of interdisciplinary research that may cut across several inter-related disciplines at the chemistry–materials science interface could be rewarding in countless ways to open up new horizons. Conceptually-novel and technologically-relevant emerging materials could be realized by capitalizing on collaborative research efforts within the chemistry community, as this report also highlight some of our personal experiences in cooperative research efforts and sharing mutual experiences in synthetic chemistry, molecular electronics, polymer chemistry, and materials engineering. The chemistry of cyclophane is under active investigations, and cyclophane chemistry will continue to blossom.

Acknowledgements

The legacy of previous generations in cyclophane chemistry is astonishing. On the occasion of PCP's 75 anniversary, this article is dedicated to all those people who have contributed to the field of Cyclophane chemistry over the last 75 years. The authors acknowledge with thanks Stefan Bräse for the support of his research at the KIT and all dedicated students/colleagues, collaboration partners and everyone who has contributed along the way in navigating the amazing "World of Cyclophanes," their names are listed as co-authors in the articles cited in this report. This compilation has emanated from the joint research efforts performed in the frame of cooperations exploring cyclophane-based precursors for engineering functional materials. Investigations on CVD polymerization were performed in the frame of "Molecular Structuring of Soft Matter" – "Der Sonderforschungsbereich SFB 1176" at KIT and at Biointerfaces Institute, University of Michigan, USA (Jörg Lahann's Labs). Investigations on π-stacked small-molecules organic emitters and TADF materials were performed in cooperation with Organic Semiconductor Centre, University of St Andrews, UK (Eli Zysman-Colman's Labs). Marcus Weck (Molecular Design Institute, NYU) is acknowledged for fruitful discussions on cyclophane-dienes based ROMP strategies during his visit to IOC at the KIT. The author is thankful to all the three anonymous reviewers that have

generously contributed vast expertise, time, energy, and provided valuable comments in the peer-review process concerning the substance of this report. The authors appreciate Marc Zastrow and Jörn Ritterbusch; Editors Advanced Functional Materials of Wiley-VCH for their kind invitation for this contribution. The author is grateful for generous support from the German Research Foundation (formally Deutsche Forschungsgemeinschaft: DFG) in the frame of "Molecular Structuring of Soft Matter" – "Der Sonderforschungsbereich SFB 1176" and DFG-funded cluster program "3D Matter Made to Order–3DMM2O" under Germany's Excellence Strategy –2082/1-390761711.

Open access funding enabled and organized by Projekt DEAL.

Conflict of Interest

The authors declare no conflict of interest.

Keywords

CVD polymerization, cyclophanes, π-stacked molecules and polymers, ROMP polymerization, supramolecular materials, surface engineering, TADF/CPL organic emitters, through-space conjugation

Received: September 26, 2023
Revised: February 11, 2024
Published online:

[1] a) P. G. Ghasemabadi, T. Yao, G. J. Bodwell, *Chem. Soc. Rev.* **2015**, *44*, 6494; b) G. P. Moss, P. A. S. Smith, D. Tavernier, *Pure Appl. Chem.* **1995**, *67*, 1307.
[2] D. J. Cram, J. M. Cram, *Acc. Chem. Res.* **1971**, *4*, 204.
[3] a) S. Misumi, T. Otsubo, *Acc. Chem. Res.* **1978**, *11*, 251; b) D. T. Longone, H. S. Chow, *J. Am. Chem. Soc.* **1970**, *92*, 994.
[4] J. Nishimura, Y. Nakamura, Y. Hayashida, T. Judo, *Acc. Chem. Res.* **2000**, *33*, 679.
[5] a) P. F. T. Schirch, V. Boekelheide, *J. Am. Chem. Soc.* **1979**, *101*, 3125; b) Y. Sekine, V. Boekelheide, *J. Am. Chem. Soc.* **1981**, *103*, 1777; c) V. Boekelheide, *Acc. Chem. Res.* **1980**, *13*, 65.
[6] a) J. Kleinschroth, H. Hopf, *Angew. Chem., Int. Ed.* **1982**, *21*, 469; b) M. Psiorz, H. Hopf, *Angew. Chem., Int. Ed.* **1982**, *21*, 623.
[7] A. de Meijere, B. König, *Synlett* **1997**, *11*, 1221.
[8] R. Gleiter, D. Kratz, *Acc. Chem. Res.* **1993**, *26*, 311.
[9] a) E. S. Hirst, R. Jasti, *J. Org. Chem.* **2012**, *77*, 10473; b) H. Omachi, Y. Segawa, K. Itami, *Acc. Chem. Res.* **2012**, *45*, 1378; c) E. R. Darzi, R. Jasti, *Chem. Soc. Rev.* **2015**, *44*, 6401; d) S. E. Lewis, *Chem. Soc. Rev.* **2015**, *44*, 2221.
[10] a) (Eds: H. Hopf, R. Gleiter), *Modern Cyclophane Chemistry*, Wiley-VCH, Weinheim **2004**; b) F. Diederich, *Cyclophanes*, Royal Society of Chemistry, Cambridge **1991**; c) (Eds: P. M. Keehn, S. M. Rosenfeld), *Cyclophanes*, Academic Press, New York, **1983**.
[11] a) C. J. Brown, A. C. Farthing, *Nature* **1949**, *164*, 915; b) M. Szwarc, *J. Chem. Phys.* **1948**, *16*, 128.
[12] D. J. Cram, H. Steinberg, *J. Am. Chem. Soc.* **1951**, *73*, 5691.
[13] a) D. J. Cram, N. L. Alligier, *J. Am. Chem. Soc.* **1955**, *77*, 6289; b) D. J. Cram, R. A. Reeves, *J. Am. Chem. Soc.* **1958**, *80*, 3094; c) D. J. Cram, M. F. Antar, *J. Am. Chem. Soc.* **1958**, *80*, 3103; d) D. J. Cram, M. F. Antar, *J. Am. Chem. Soc.* **1958**, *80*, 3109; e) K. C. Dewhirst, D. J. Cram, *J. Am. Chem. Soc.* **1958**, *80*, 3115; f) D. J. Cram, J. Wechter, R. W. Kierstead, *J. Am. Chem. Soc.* **1958**, *80*, 3126; g) D. J. Cram, R. H. Bauer, *J. Am. Chem. Soc.* **1959**, *81*, 5971; h) D. J. Cram, R. H. Bauer, N. L. Allinger, R. A. Reeves, W. J. Wechter, E. Heilbronner, *J. Am. Chem. Soc.* **1959**, *81*, 5977; i) L. A. Singer, D. J. Cram, *J. Am. Chem. Soc.* **1963**, *85*, 1080; j) D. J. Cram, L. A. Singer, *J. Am. Chem. Soc.* **1963**, *85*, 1084; k) H. J. Reich, D. J. Cram, *J. Am. Chem. Soc.* **1967**, *89*, 3078; l) H. J. Reich, D. J. Cram, *J. Am. Chem. Soc.* **1968**, *90*, 1365; m) H. J. Reich, D. J. Cram, *J. Am. Chem. Soc.* **1969**, *91*, 3505; n) H. J. Reich, D. J. Cram, *J. Am. Chem. Soc.* **1969**, *91*, 3517; o) H. J. Reich, D. J. Cram, *J. Am. Chem. Soc.* **1969**, *91*, 3527; p) H. J. Reich, D. J. Cram, *J. Am. Chem. Soc.* **1969**, *91*, 3534; q) M. Sheehan, D. J. Cram, *J. Am. Chem. Soc.* **1969**, *91*, 3544; r) M. Sheehan, D. J. Cram, *J. Am. Chem. Soc.* **1969**, *91*, 3553; s) R. E. Singler, R. C. Helgeson, D. J. Cram, D. J. Cram, *J. Am. Chem. Soc.* **1970**, *92*, 7625; t) R. B. Hornby, E. A. Truesdale, H. J. Reich, M. H. Delton, J. M. Cram, *Tetrahedron* **1974**, *30*, 1757.
[14] a) C. J. Brown, *J. Chem. Soc.* **1953**, 3265, https://pubs.rsc.org/en/content/articlelanding/1953/jr/jr9530003265; b) H. Hope, J. Bernstein, K. N. Trueblood, *Acta Crystallogr.* **1972**, *28*, 1733; c) D. K. Lonsdale, H. J. Milledge, K. V. K. Rao, *Proc. R. Soc. London A* **1960**, *255*, 82; d) C. L. Coulter, K. N. Trueblood, *Acta Crystallogr.* **1963**, *16*, 667; e) P. K. Gantzel, K. N. Trueblood, *Acta Crystallogr.* **1965**, *18*, 958; f) S. Grimme, *Chem. - Eur. J.* **2004**, *10*, 3423; g) H. Wolf, D. Leusser, M. R. V. Jorgensen, R. H. Irmer, Y. S. Chen, E. W. Scheidt, W. Scherer, B. B. Iversen, D. Stalke, *Chem. - Eur. J.* **2014**, *20*, 7048; h) S. M. Bachrach, *J. Phys. Chem. A* **2011**, *115*, 2396; i) H. Dodziuk, S. Szymanski, J. Jazwi nski, M. Ostrowski, T. B. Demissie, K. Ruud, P. Kus, H. Hopf, S. T. Lin, *J. Phys. Chem. A* **2011**, *115*, 10638; j) T. Itoh, F. Kondo, T. Uno, M. Kubo, N. Tohnai, M. Miyata, *Cryst. Growth Des.* **2017**, *17*, 3606; k) Z. A. Starikova, I. V. Fedyanin, M. Y. Antipin, *Russ. Chem. Bull.* **2004**, *53*, 1779; l) A. M. Castro, *Chem. Phys. Lett.* **2011**, *517*, 113; m) K. A. Lyssenko, M. Y. Antipin, D. Y. Antonov, *ChemPhysChem* **2003**, *4*, 817; n) S. E. Walden, D. T. Glatzhofer, *J. Phys. Chem. A* **1997**, *101*, 8233; o) D. Henseler, G. Hohlneicher, *J. Phys. Chem. A* **1999**, *103*, 1160; p) S. E. Walden, D. T. Glatzhofer, *J. Phys. Chem. A* **1999**, *103*, 1162; q) S. Canuto, M. C. Zerner, *J. Am. Chem. Soc.* **1990**, *112*, 2114.
[15] a) Z. Hassan, E. Spuling, D. M. Knoll, J. Lahann, S. Bräse, *Chem. Soc. Rev.* **2018**, *47*, 6947; b) Z. Hassan, S. Bräse, *Chem. - Eur. J.* **2021**, *27*, 15021; c) S. Bräse, S. Dahmen, S. Höfener, F. Lauterwasser, M. Kreis, R. E. Ziegert, *Synlett* **2004**, *15*, 2647.
[16] a) P. J. Pye, K. Rossen, R. A. Reamer, N. N. Tsou, R. P. Volante, P. J. Reider, *J. Am. Chem. Soc.* **1997**, *119*, 6207; b) A. Togni, C. Breutel, A. Schnyder, F. Spindler, H. Landert, A. Tijani, *J. Am. Chem. Soc.* **1994**, *116*, 4062; c) H. Liang, W. Guo, J. Li, J. Jiang, J. Wang, *Angew. Chem., Int. Ed.* **2022**, *61*, e202204926.
[17] a) V. Rozenberg, T. Danilova, E. Sergeeva, E. Vorontsov, Z. Starikova, K. Lysenko, Y. Belokon, *Eur. J. Org. Chem.* **2000**, 3295; b) V. Rozenberg, E. Sergeeva, H. Hopf, in *Modern Cyclophane Chemistry*, (Eds.: R. Gleiter, H. Hopf), Wiley-VCH, Weinheim **2004**.
[18] a) G. J. Rowlands, *Isr. J. Chem.* **2012**, *52*, 60; b) G. J. Rowlands, *Org. Biomol. Chem.* **2008**, *6*, 1527; c) S. E. Gibson, J. D. Knight, *Org. Biomol. Chem.* **2003**, *1*, 1256.
[19] a) J. F. Schneider, R. Fröhlich, J. Paradies, *Isr. J. Chem.* **2012**, *52*, 76; b) J. Paradies, *Synthesis* **2011**, *2011*, 3749.
[20] S. Felder, S. Wu, J. Brom, L. Micouin, E. Benedetti, *Chirality* **2021**, *33*, 506.
[21] a) P. An, Y. Huo, Z. Chen, C. Song, Y. Ma, *Org. Biomol. Chem.* **2017**, *15*, 3202; b) Z. Niu, J. Chen, Z. Chen, M. Ma, C. Song, Y. Ma, *J. Org. Chem.* **2015**, *80*, 602; c) Y. Ma, C. Song, C. Ma, Z. Sun, Q. Chai, M. B. Andrus, *Angew. Chem., Int. Ed.* **2003**, *42*, 5871; d) L. Zhao, Y. Ma, F. He, W. Duan, J. Chen, C. Song, *J. Org. Chem.* **2013**, *78*, 1677.
[22] a) C. Bolm, D. K. Whelligan, *Adv. Synth. Catal.* **2006**, *348*, 2093; b) D. K. Whelligan, C. Bolm, *J. Org. Chem.* **2006**, *71*, 4609.
[23] a) S. Bräse, (Ed: D. Enders) *Asymmetric Synthesis with Chemical and Biological Methods*, Wiley-VCH, Weinheim **2007**; b) S. Bräse,

(Eds: M. Christmann, S. Bräse), *Asymmetric Synthesis: The Essentials*, Wiley-VCH, Weinheim **2006**.

[24] a) Y. Q. Bai, X. W. Wang, B. Wu, X. Q. Wang, R. Z. Liao, M. Li, Y. G. Zhou, *ACS Catal.* **2023**, *13*, 9829; b) Z. H. Zhu, Y. X. Ding, Y. G. Zhou, *Chem. Commun.* **2022**, *58*, 3973; c) Z. H. Zhu, Y. X. Ding, B. Wu, Y. G. Zhou, *Org. Lett.* **2021**, *23*, 7166; d) Z. B. Zhao, J. Wang, Z. H. Zhu, M. W. Chen, Y. G. Zhou, *Org. Lett.* **2021**, *23*, 9112; e) Z. H. Zhu, Y. X. Ding, B. Wu, Y. G. Zhou, *Chem. Sci.* **2020**, *11*, 10220.

[25] H. E. Winberg, F. S. Fawcett, W. E. Mochel, C. W. Theobald, *J. Am. Chem. Soc.* **1960**, *82*, 1428.

[26] a) S. Oßwald, C. Zippel, Z. Hassan, M. Nieger, S. Bräse, *RSC Adv.* **2022**, *12*, 3309; b) R. S. Givens, R. J. Olsen, P. L. Wylie, *J. Org. Chem.* **1979**, *44*, 1608.

[27] a) T. A. Shear, F. Lin, L. N. Zakharov, D. W. Johnson, *Angew. Chem., Int. Ed.* **2020**, *59*, 1496; b) N. M. Phan, E. G. Percastegui, D. W. Johnson, *ChemPlusChem* **2020**, *85*, 1270.

[28] R. Filler, G. L. Cantrell, D. Wolanin, S. M. Naqvi, *J. Fluorine Chem.* **1986**, *30*, 399.

[29] a) W. R. Dolbier, X. X. Rong, Y. Xu, W. F. Beach, *J. Org. Chem.* **1997**, *62*, 7500; b) A. J. Roche, W. R. Dolbier, *J. Org. Chem.* **1999**, *64*, 9137; c) W. R Dolbier, J. X. Duan, A. J. Roche, *Org. Lett.* **2000**, *2*, 1867; d) A. J. Roche, W. R. Dolbier, *J. Org. Chem.* **2000**, *65*, 5282; e) W. R. Dolbier, W. F. Beach, *J. Fluorine Chem.* **2003**, *122*, 97; f) A. Davila, J. O. Escobedo, M. W. Read, F. R. Fronczek, R. M. Strongin, *Tetrahedron Lett.* **2001**, *42*, 3555; g) A. J. Roche, J. X. Duan, W. R. Dolbier, K. A. Abboud, *J. Org. Chem.* **2001**, *66*, 7055; h) C. Hicks, B. Duffy, G. C. Hargaden, *Org. Chem. Front.* **2014**, *1*, 716; i) T. Itoh, S. Okuoka, M. Kubo, S. Iwatsuki, *J. Polym. Sci., Part A: Polym. Chem.* **1995**, *33*, 359; j) A. J. Roche, A. A. Marchione, *Magn. Reson. Chem.* **2012**, *50*, 809; k) A. J. Roche, S. A. Rabinowitz, K. A. Cox, *Tetrahedron: Asymmetry* **2013**, *24*, 1382; l) I. Ghiviriga, F. Dulong, W. R. Dolbier, *Magn. Reson. Chem.* **2009**, *47*, 313; m) W. R. Dolbier, J. X. Duan, A. J. Roche, US6392097B1, **2001**.

[30] a) O. Reiser, A. de Meijere, *Angew. Chem., Int. Ed.* **1987**, *26*, 1277; b) O. Reiser, B. Konig, K. Meerholz, J. Heinze, T. Wellauer, F. Gerson, R. Frim, M. Rabinovitz, A. de Meijere, *J. Am. Chem. Soc.* **1993**, *115*, 3511.

[31] E. T. Csányi, H. D. Höhnk, *J. Mol. Catal.* **1992**, *76*, 101.

[32] a) T. Otsubo, V. Boekelheide, *Tetrahedron Lett.* **1975**, *16*, 3881; b) M. Montanari, A. Bugana, A. K. Sharma, D. Pasini, *Org. Biomol. Chem.* **2011**, *9*, 5018; c) F. Invernizzi, A. Nitti, D. Pasini, *Phosphorus Sulfur Silicon Relat. Elem.* **2021**, *196*, 189; d) B. J. Lidster, D. R. Kumar, A. M. Spring, C. Y. Yu, M. Helliwell, J. Raftery, M. L. Turner, *Org. Biomol. Chem.* **2016**, *14*, 6079.

[33] J. J. P. Kramer, M. Nieger, S. Bräse, *Eur. J. Org. Chem.* **2013**, *3*, 541.

[34] S. J. Koehler, J. Hu, E. Elacqua, *Synlett* **2020**, *31*, 1435.

[35] a) Z. Hassan, E. Spuling, D. M. Knoll, S. Bräse, *Angew. Chem., Int. Ed.* **2020**, *59*, 2156; b) K. J. Weiland, A. Gallego, M. Mayor, *Eur. J. Org. Chem.* **2019**, 3073; c) O. R. P. David, *Tetrahedron* **2012**, *68*, 8977.

[36] a) A. de Meijere, B. Stulgies, K. Albrecht, K. Rauch, H. A. Wegner, H. Hopf, L. T. Scott, L. Eshdat, I. Aprahamian, M. Rabinovitz, *Pure Appl. Chem.* **2006**, *78*, 813; b) H. Hopf, *Angew. Chem., Int. Ed.* **2008**, *47*, 9808; c) H. Hopf, *Isr. J. Chem.* **2012**, *52*, 18.

[37] A. Marrocchi, I. Tomasi , L. Vaccaro, *Isr. J. Chem.* **2012**, *52*, 41.

[38] a) A. Batra, G. Kladnik, H. Vázquez, J. S. Meisner, L. Floreano, C. Nuckolls, D. Cvetko, A. Morgante, L. Venkataraman, *Nat. Commun.* **2012**, *3*, 1086; b) S. T. Schneebeli, M. Kamenetska, Z. Cheng, R. Skouta, R. A. Friesner, L. Venkataraman, R. Breslow, *J. Am. Chem. Soc.* **2011**, *133*, 2136; c) I. Majerz, T. Dziembowska, *J. Phys. Chem. A* **2016**, *120*, 8138.

[39] a) G. P. Bartholomew, G. C. Bazan, *Acc. Chem. Res.* **2001**, *34*, 30; b) G. C. Bazan, *J. Org. Chem.* **2007**, *72*, 8615.

[40] a) W. J. Oldham, Y. J. Miao, R. J. Lachicotte, G. C. Bazan, *J. Am. Chem. Soc.* **1998**, *120*, 419; b) G. C. Bazan, W. J. Oldham, R. J. Lachicotte, S. Tretiak, V. Chernyak, S. Mukamel, *J. Am. Chem. Soc.* **1998**, *120*, 9188; c) J. Zyss, I. Ledoux, S. Volkov, V. Chernyak, S. Mukamel, G. P. Bartholomew, G. C. Bazan, *J. Am. Chem. Soc.* **2000**, *122*, 11956; d) G. P. Bartholomew, G. C. Bazan, *J. Am. Chem. Soc.* **2002**, *124*, 5183; e) J. W. Hong, B. S. Gaylord, G. C. Bazan, *J. Am. Chem. Soc.* **2002**, *124*, 11868; f) G. P. Bartholomew, I. Ledoux, S. Mukamel, G. C. Bazan, J. Zyss, *J. Am. Chem. Soc.* **2002**, *124*, 13480; g) E. S. Baker, J. W. Hong, J. Gidden, G. P. Bartholomew, G. C. Bazan, M. T. Bowers, *J. Am. Chem. Soc.* **2004**, *126*, 6255; h) G. P. Bartholomew, M. Rumi, S. J. K. Pond, J. W. Perry, S. Tretiak, G. C. Bazan, *J. Am. Chem. Soc.* **2004**, *126*, 11529; i) W. Leng, J. Grunden, G. P. Bartholomew, G. C. Bazan, A. M. Kelley, *J. Phys. Chem. A* **2004**, *108*, 10050; j) J. W. Hong, H. Y. Woo, B. Liu, G. C. Bazan, *J. Am. Chem. Soc.* **2005**, *127*, 7435.

[41] G. Hong, X. Gan, C. Leonhardt, Z. Zhang, J. Seibert, J. M. Busch, S. Bräse, *Adv. Mater.* **2021**, *33*, 2005630.

[42] a) H. Uoyama, K. Goushi, K. Shizu, H. Nomura, C. Adachi, *Nature* **2012**, *492*, 234; b) M. Y. Wong, E. Z. Colman, *Adv. Mater.* **2017**, *29*, 1605444.

[43] a) S. L. Buchwald, W. Huang, *US9972791B2*, **2018**. b) J. H. Yang, K. J. Yoon, H. J. Noh, D. W. Yoon, I. A. Shin, J. Y. Kim, EP3029753B1, **2015**

[44] a) J. M. Teng, D. W. Zhang, C. F. Chen, *ChemPhotoChem* **2022**, *6*, 20210022; b) J. Li, P. Shen, Z. Zhao, B. Z. Tang, *CCS Chem.* **2019**, *1*, 181; c) W. Liu, H. Li, Y. Huo, Q. Yao, W. Duan, *Molecules* **2023**, *28*, 2891.

[45] E. Spuling, N. Sharma, I. D. W. Samuel, E. Z. Colman, S. Bräse, *Chem. Commun.* **2018**, *54*, 9278.

[46] M. Y. Zhang, Z. Y. Li, B. Lu, Y. Wang, Y. D. Ma, C. H. Zhao, *Org. Lett.* **2018**, *20*, 6868.

[47] M. Y. Zhang, X. Liang, D. N. Ni, D. H. Lia, Q. Peng, C. H. Zhao, *Org. Lett.* **2021**, *23*, 2.

[48] N. Sharma, E. Spuling, C. M. Mattern, W. Li, O. Fuhr, Y. Tsuchiya, C. Adachi, S. Bräse, I. D. W. Samuel, E. Z. Colman, *Chem. Sci.* **2019**, *10*, 6689.

[49] A. K. Gupta, Z. Zhang, E. Spuling, K. Kaczmarek, Y. Wang, Z. Hassan, I. D. W. Samuel, S. Bräse, E. Z. Colman, *Mater. Adv.* **2021**, *2*, 6684.

[50] C. Liao, Y. Zhang, S. H. Ye, W. H. Zheng, *ACS Appl. Mater. Interfaces* **2021**, *13*, 25186.

[51] D. W. Zhang, J. M. Teng, Y. F. Wang, X. N. Han, M. Li, C. F. Chen, *Mater. Horiz.* **2021**, *8*, 3417.

[52] S. M. Suresh, D. Hall, D. Beljonne, Y. Olivier, E. Z. Colman, *Adv. Funct. Mater.* **2020**, *30*, 1908677

[53] X. J. Liao, D. Pu, L. Yuan, J. Tong, S. Xing, Z. H. Tu, J. L. Zuo, W. H. Zheng, Y. X. Zheng, *Angew. Chem., Int. Ed.* **2023**, *62*, e202217045.

[54] X. Liang, T. T. Liu, Z. P. Yan, Y. Zhou, J. Su, X. F. Luo, Z. G. Wu, Y. Wang, Y. X. Zheng, J. L. Zuo, *Angew. Chem., Int. Ed.* **2019**, *58*, 17220.

[55] Z. Zhang, S. Diesing, E. Crovini, A. Kumar Gupta, E. Spuling, X. Gan, O. Fuhr, M. Nieger, Z. Hassan, I. D. W. Samuel, S. Bräse, E. Z. Colman, *Org. Lett.* **2021**, *23*, 6697.

[56] a) F. Salhi, D. M. Collard, *Adv. Mater.* **2003**, *15*, 81; b) S. P. Jagtap, D. M. Collard, *J. Am. Chem. Soc.* **2010**, *132*, 12208; c) S. Mukhopadhyay, S. P. Jagtap, V. Coropceanu, J. L. Bredas, D. M. Collard, *Angew. Chem., Int. Ed.* **2012**, *51*, 11629; d) S. P. Jagtap, D. M. Collard, *Polym. Chem.* **2012**, *3*, 463; e) D. M. Collard, in *π-Stacked Polymers and Molecules, Theory, Synthesis and Properties*, (Ed.: T. Nakano), Springer, Japan **2014**.

[57] a) Y. Morisaki, Y. Chujo, *Bull. Chem. Soc. Jpn.* **2019**, *92*, 265; b) Y. Morisaki, Y. Chujo, *Chem. Lett.* **2012**, *41*, 840; c) Y. Morisaki, Y. Chujo, *Polym. Chem.* **2011**, *2*, 1249; d) Y. Morisaki, Y. Chujo, *Bull. Chem. Soc. Jpn.* **2009**, *82*, 1070; e) Y. Morisaki, Y. Chujo, *Angew. Chem., Int. Ed.* **2006**, *45*, 6430; f) Y. Morisaki, Y. Chujo, *Prog. Polym. Sci.* **2008**, *33*, 346.

[58] a) Y. Morisaki, M. Gon, T. Sasamori, N. Tokitoh, Y. Chujo, *J. Am. Chem. Soc.* **2014**, *136*, 3350; b) G. Namba, Y. Mimura, Y. Imai, R.

Inoue, Y. Morisaki, *Chem. - Eur. J.* **2020**, *26*, 14871; c) Y. Sasai, R. Inoue, Y. Morisaki, *Bull. Chem. Soc. Jpn.* **2020**, *93*, 1193.
[59] a) M. Gon, Y. Morisaki, Y. Chujo, *Eur. J. Org. Chem.* **2015**, *2015*, 7756; b) Y. Morisaki, K. Inoshita, Y. Chujo, *Chem. - Eur. J.* **2014**, *20*, 8386.
[60] a) M. Gon, H. Kozuka, Y. Morisaki, Y. Chujo, *Asian J. Org. Chem.* **2016**, *5*, 353; b) M. Gon, Y. Morisaki, Y. Chujo, *J. Mater. Chem. C* **2015**, *3*, 521.
[61] a) A. Morisaki, R. Inoue, Y. Morisaki, *Chem. - Eur. J.* **2023**, *29*, e202203533; b) Y. Morisaki, R. Hifumi, L. Lin, K. Inoshita, Y. Chujo, *Polym. Chem.* **2012**, *3*, 2727; c) Y. Morisaki, L. Lin, Y. Chujo, *Polym. Bull.* **2009**, *62*, 737; d) Y. Morisaki, N. Wada, M. Arita, Y. Chujo, *Polym. Bull.* **2009**, *62*, 305; e) Y. Morisaki, T. Murakami, T. Sawamura, Y. Chujo, *Macromolecules* **2009**, *42*, 3656; f) Y. Morisaki, T. Murakami, Y. Chujo, *Macromolecules* **2008**, *41*, 5960.
[62] Y. Morisaki, Y. Chujo, *Bull. Chem. Soc. Jpn.* **2005**, *78*, 288.
[63] a) Y. Morisaki, in *Circularly Polarized Luminescence of Isolated Small Organic Molecules*, (Ed: T. Mori), Springer, Singapore, **2020**; b) Y. Morisaki, Y. Chujo, in *π-Stacked Polymers and Molecules, Theory, Synthesis and Properties*, (Ed: T. Nakano), Springer, Japan **2014**.
[64] a) E. Sidler, P. Zwick, C. Kress, K. Reznikova, O. Fuhr, D. Fenske, M. Mayor, *Chem. - Eur. J.* **2022**, *28*, e202201764; b) C. Kress, E. Sidler, P. Downey, P. Zwick, O. Fuhr, D. Fenske, S. Bernhard, M. Mayor, *Chem. - Eur. J.* **2024**, *30*, e202303798.
[65] a) K. J. Weiland, T. Brandl, K. Atz, A. Prescimone, D. Häussinger, T. Solomek, M. Mayor, *J. Am. Chem. Soc.* **2019**, *141*, 2104; b) K. J. Weiland, N. Münch, W. Gschwind, D. Häussinger, M. Mayor, *Helv. Chim. Acta* **2019**, *102*, 1800.
[66] a) M. Hasegawa, K. Kobayakawa, Y. Nojima, Y. Mazaki, *Org. Biomol. Chem.* **2019**, *17*, 8822; b) M. Hasegawa, Y. Ishida, H. Sasaki, S. Ishioka, K. Usui, N. Hara, M. Kitahara, Y. Imai, Y. Mazaki, *Chem. - Eur. J.* **2021**, *27*, 16225; c) M. Hasegawa, Y. Ishida, H. Sasaki, S. Ishioka, K. Usui, N. Hara, M. Kitahara, Y. Imai, Y. Mazaki, *Chem. - Eur. J.* **2017**, *23*, 3267; d) L. Ren, Y. Han, X. Hou, Y. Ni, J. Wu, *Chem. - Eur. J.* **2024**, *30*, e202304088.
[67] J. He, M. Yu, M. Pang, Y. Fan, Z. Lian, Y. Wang, W. Wang, Y. Liu, H. Jiang, **2022**, *Chem. - Eur. J. 28*, e202103832.
[68] a) Y. Fan, J. He, L. Liu, G. Liu, S. Guo, Z. Lian, X. Li, W. Guo, X. Chen, Y. Wang, H. Jiang, *Angew. Chem., Int. Ed.* **2023**, *64*, e202304623; b) J. He, M. H. Yu, Z. Lian, Y. Q. Fan, S. Z. Guo, X. N. Li, Y. Wang, W. G. Wang, Z. Y. Cheng, H. Jiang, *Chem. Sci.* **2023**, *14*, 4426; c) Y. Wu, G. Zhuang, S. Cui, Y. Zhou, J. Wang, Q. Huang, P. Du, *Chem. Commun.* **2019**, *55*, 14617.
[69] D. Han, X. Yang, J. Han, J. Zhou, T. Jiao, P. Duan, *Nat. Commun.* **2020**, *11*, 5659.
[70] a) M. Mohanan, H. Ahmad, P. Ajayan, P. K. Pandey, B. M. Calvert, X. Zhang, F. Chen, S. J. Kim, S. Kundu, N. Gavvalapalli, *Chem. Sci.* **2023**, *14*, 5510; b) F. Hameed, M. Mohanan, N. Ibrahim, C. Ochonma, J. R. Lopez, N. Gavvalapalli, *Macromolecules* **2023**, *56*, 3421; c) S. Chaudhuri, M. Mohanan, A. V. Willems, J. A. Bertke, N. Gavvalapalli, *Chem. Sci.* **2019**, *10*, 5976.
[71] a) C. S. Wang, Y. C. Wei, K. H. Chang, P. T. Chou, Y. T. Wu, *Angew. Chem., Int. Ed.* **2019**, *58*, 10158; b) C. S. Wang, Y. C. Wei, M. L. Pan, C. H. Wu, P. T. Chou, Y. T. Wu, *Chem. - Eur. J.* **2021**, *27*, 8678.
[72] a) K. Mutoh, Y. Nakagawa, A. Sakamoto, Y. Kobayashi, J. Abe, *J. Am. Chem. Soc.* **2015**, *137*, 5674; b) Y. Kobayashi, T. Katayama, T. Yamane, K. Setoura, S. Ito, H. Miyasaka, J. Abe, *J. Am. Chem. Soc.* **2016**, *138*, 5930; c) Y. Kobayashi, J. Abe, *Adv. Opt. Mater.* **2016**, *4*, 1354; d) Y. Kobayashi, K. Mutoh, J. Abe, *J. Phys. Chem. Lett.* **2016**, *7*, 3666; e) K. Mutoh, M. Sliwa, E. Fron, J. Hofkens, J. Abe, *J. Mater. Chem. C* **2018**, *6*, 9523; f) A. Perrier, D. Jacquemin, *Tetrahedron* **2017**, *73*, 4936.
[73] a) M. R. Rapp, W. Leis, F. Zinna, L. Di Bari, T. Arnold, B. Speiser, M. Seitz, H. F. Bettinger, *Chem. - Eur. J.* **2022**, *28*, e202104161; b) H. F. Bettinger, R. Einholz, A. Göttler, M. Junge, M. S. Sättele, A. Schnepf, C. Schrenk, S. Schundelmeier, B. Speiser, *Org. Chem. Front.* **2017**, *4*, 853; c) R. Bula, M. Fingerle, A. Ruff, B. Speiser, C. M. Mössmer, H. F. Bettinger, *Angew. Chem., Int. Ed.* **2013**, *52*, 11647.
[74] D. B. Amabilino, P. A. Gale, *Chem. Soc. Rev.* **2017**, *46*, 2376.
[75] a) L. Brunsveld, B. J. B. Folmer, E. W. Meijer, R. P. Sijbesma, *Chem. Rev.* **2001**, *101*, 4071; b) J. M. Lehn, *Chem. Soc. Rev.* **2017**, *46*, 2378
[76] W. R. Henderson, R. K. Castellano, *Polym. Int.* **2021**, *70*, 897.
[77] a) D. E. Fagnani, M. J. Meese, K. A. Abboud, R. K. Castellano, *Angew. Chem., Int. Ed.* **2016**, *55*, 10726; b) D. B. Korlepara, W. R. Henderson, R. K. Castellano, S. Balasubramanian, *Chem. Commun.* **2019**, *55*, 3773; c) W. R. Henderson, A. Kumar, K. A. Abboud, R. K. Castellano, *Chem. - Eur. J.* **2020**, *72*, 17588.
[78] W. R. Henderson, Y. Zhu, D. E. Fagnani, G. Liu, K. A. Abboud, R. K. Castellano, *J. Org. Chem.* **2020**, *85*, 1158.
[79] W. R. Henderson, G. Liu, K. A. Abboud, R. K. Castellano, *J. Am. Chem. Soc.* **2021**, *143*, 12688.
[80] O. Oki, H. Yamagishi, Y. Morisaki, R. Inoue, K. Ogawa, N. Miki, Y. Norikane, H. Sato, Y. Yamamoto, *Science* **2022**, *377*, 673.
[81] a) T. S. I. M.-O. Frameworks, H. C. Zhou, S. Kitagawa, *Chem. Soc. Rev.* **2014**, *43*, 5415; b) A. G. Slater, A. I. Cooper, *Science* **2015**, *348*, aaa8075; c) M. J. Kalmutzki, N. Hanikel, O. M. Yaghi, *Sci. Adv.* **2018**, *4*, eaat9180.
[82] W. Gong, H. Xie, K. B. Idrees, F. A. Son, Z. Chen, F. Sha, Y. Liu, Y. Cui, O. K. Farha, *J. Am. Chem. Soc.* **2022**, *144*, 1826.
[83] a) H. Jiang, W. Zhang, B. Hou, Y. Liu, Y. Cui, *CCS Chem.* **2023**, *5*, 1635; b) M. L. Birsa, H. Hopf, P. G. Jones, L. G. Sarbu, L. G. Bahrin, *Materials* **2023**, *16*, 4051.
[84] Z. Lian, J. He, L. Liu, Y. Fan, X. Chen, H. Jiang, *Nat. Commun.* **2023**, *14*, 2752.
[85] a) T. Friscic, E. Elacqua, S. Dutta, S. M. Oburn, L. R. MacGillivray, *Cryst. Growth Des.* **2020**, *20*, 2584; b) G. S. Papaefstathiou, T. Friscic, L. R. MacGillivray, *J. Am. Chem. Soc.* **2005**, *127*, 14160; c) E. Elacqua, P. T. Jurgens, J. Baltrusaitis, L. R. MacGillivray, *CrystEngComm* **2012**, *14*, 7567.
[86] X. Xue, J. Wang, Q. Zhu, Y. Xuea, H. Liu, *Dalton Trans.* **2021**, *50*, 1374.
[87] a) M. Cakici, Z. G. Gu, M. Nieger, J. Bürck, L. Heinke, S. Bräse, *Chem. Commun.* **2015**, *51*, 4796; b) J. Anhäuser, R. Puttreddy, Y. Lorenz, A. Schneider, M. Engeser, K. Rissanen, A. Lützen, *Org. Chem. Front.* **2019**, *6*, 1226; c) L. Volbach, N. Struch, F. Bohle, F. Topic, G. Schnakenburg, A. Schneider, K. Rissanen, S. Grimme, A. Lützen, *Chem. - Eur. J.* **2020**, *26*, 3335; d) G. M. Eppler, F. Topic, G. Schnakenburg, K. Rissanen, A. Lützen, *Eur. J. Inorg. Chem.* **2014**, 2495; e) D. R. Martir, L. Delforce, D. B. Cordes, A. M. Z. Slawin, S. L. Warriner, D. Jacquemin, E. Z. Colman, *Inorg. Chem. Front.* **2020**, *7*, 232.
[88] Z. Shan, M. Wu, Z. Gu, Y. Nishiyama, G. Zhang, **2021**, *Chem. Commun. 57*, 9236.
[89] a) X. Deng, K. C. K. Cheng, J. Lahann, in *CVD Polymers: Fabrication of Organic Surfaces and Devices*, (Ed: K. K. Gleason), Wiley-VCH, Weinheim, Germany **2015**; b) D. Klee, N. Weis, J. Lahann in *Modern Cyclophane Chemistry*, (Eds.: R. Gleiter, H. Hopf), Wiley-VCH, Weinheim, **2004**; c) W. F. Gorham, *J. Polym. Sci., Part A-1: Polym. Chem.* **1966**, *4*, 3027.
[90] *CVD Polymers: Fabrication of Organic Surfaces and Devices*, (Ed: K. K. Gleason), Wiley-VCH, Weinheim **2015**.
[91] a) W. S. Trahanovsky, S. P. Lorimor, *J. Org. Chem.* **2006**, *71*, 1784; b) K. Smalara, A. Gieldon, M. Bobrowski, J. Rybicki, C. Czaplewski, *J. Phys. Chem. A* **2010**, *114*, 4296.
[92] a) L. Sun, G. Yuan, L. Gao, J. Yang, M. Chhowalla, M. H. Gharahcheshmeh, K. K. Gleason, Y. S. Choi, B. H. Hong, Z. Liu, *Nat. Rev. Methods Primers* **2021**, *1*, 5; b) T. Moss, A. Greiner, *Adv. Mater. Interfaces* **2020**, *11*, 1901858; c) A. Khlyustova, Y. Cheng, R. Yang, *J. Mater. Chem. B* **2020**, *8*, 6588; d) M. Koenig, J. Lahann, *Beilstein J. Nanotechnol.* **2017**, *8*, 2219; e) B. J. Kim, E. Meng, *Polym. Adv. Technol.* **2016**, *27*, 564.

[93] a) T. Itoh, *Prog. Polym. Sci.* **2001**, *26*, 1019; b) W. F. Gorham, Y. L. Yeh, *J. Org. Chem.* **1969**, *34*, 2366.
[94] a) F. B. Le Gall, C. Hussal, J. Kramer, K. Cheng, R. Kumar, T. Eyster, A. Baek, V. Trouillet, M. Nieger, S. Bräse, J. Lahann, *Chem. - Eur. J.* **2017**, *23*, 13342; b) T. Itoh, T. Iwasaki, M. Kubo, S. Iwatsuki, *Polym. Bull.* **1995**, *35*, 307.
[95] a) H. Y. Chen, J. Lahann, *Langmuir* **2011**, *27*, 34; b) A. M. Ross, J. Lahann, *Annu. Rev. Chem. Biomol. Eng.* **2015**, *6*, 161; c) J. Lahann, I. S. Choi, J. Lee, K. F. Jensen, R. Langer, *Angew. Chem., Int. Ed.* **2001**, *40*, 3166.
[96] M. H. Alonso, T. J. McCarthy, *Langmuir* **2004**, *20*, 9184.
[97] H. Nandivada, H. Y. Chen, L. Bondarenko, J. Lahann, *Angew. Chem., Int. Ed.* **2006**, *45*, 3360.
[98] a) F. Y. Chou, T. C. Ramli, C. Y. Lee, S. M. Hua, J. Christy, H. Y. Chen, *Org. Mater.* **2023**, *5*, 118; b) Z. Hassan, D. Varadharajan, C. Zippel, S. Begum, J. Lahann, S. Bräse, *Adv. Mater.* **2022**, *34*, 2201761.
[99] a) X. Deng, C. Friedmann, J. Lahann, *Angew. Chem., Int. Ed.* **2011**, *50*, 6522; b) M. Y. Tsai, Y. C. Chen, T. J. Lin, Y. C. Hsu, C. Y. Lin, R. H. Yuan, J. Yu, M. S. Teng, M. Hirtz, M. H. C. Chen, C. H. Chang, H. Y. Chen, *Adv. Funct. Mater.* **2014**, *24*, 2281.
[100] a) A. Ross, H. Durmaz, K. Cheng, X. Deng, Y. Liu, J. Oh, Z. Chen, J. Lahann, *Langmuir* **2015**, *31*, 5123; b) F. Bally, K. Cheng, H. Nandivada, X. Deng, A. M. Ross, A. Panades, J. Lahann, *ACS Appl. Mater. Interfaces* **2013**, *5*, 9262; c) A. L. Winkler, M. Koenig, A. Welle, V. Trouillet, D. Kratzer, C. Hussal, J. Lahann, C. Lee-Thedieck, *Biomacromolecules* **2017**, *18*, 3089.
[101] a) H. Y. Chen, T. J. Lin, M. Y. Tsai, C. T. Su, R. H. Yuan, C. C. Hsieh, Y. J. Yang, C. C. Hsu, H. M. Hsiao, Y. C. Hsu, *Chem. Commun.* **2013**, *49*, 4531; b) C. Y. Wu, C. W. Chang, R. H. Yuan, Y. C. Chiang, J. T. Chen, D. Y. Kang, H. Y. Chen, *Nanoscale* **2017**, *9*, 14787.
[102] F. Xie, X. Deng, D. Kratzer, K. C. K. Cheng, C. Friedmann, S. Qi, L. Solorio, J. Lahann, *Angew. Chem., Int. Ed.* **2017**, *56*, 203.
[103] a) K. C. K. Cheng, M. A. B. Pantoja, Y. K. Kim, J. V. Gregory, F. Xie, A. de France, C. Hussal, K. Sun, N. L. Abbott, J. Lahann, *Science* **2018**, *362*, 804; b) M. A. B. Pantoja, N. L. Abbott, K. Cheng, J. Lahann, US10907038B2, **2017**.
[104] a) D. Varadharajan, K. Nayani, C. Zippel, E. Spuling, K. C. Cheng, S. Sarangarajan, S. Roh, J. Kim, V. Trouillet, S. Bräse, N. L. Abbott, J. Lahann, *Adv. Mater.* **2021**, *34*, 2108386; b) S. Roh, J. Kim, D. Varadharajan, J. Lahann, N. L. Abbott, *Adv. Funct. Mater.* **2022**, *32*, 2200830.
[105] C. Zippel, Z. Hassan, A. Q. Parsa, J. Hohmann, S. Bräse, *Adv. Synth. Catal.* **2021**, *363*, 2861.
[106] M. C. Demirel, S. Boduroglu, M. Cetinkaya, A. Lakhtakia, *Langmuir* **2007**, *23*, 5861.
[107] S. Begum, F. Behboodi-Sadabad, Y. Pramudya, C. Dolle, M. Kozlowska, Z. Hassan, C. Mattern, S. Gorji, S. Heißler, A. Welle, M. Koenig, W. Wenzel, Y. M. Eggeler, S. Bräse, J. Lahann, M. Tsotsalas, *Chem. Mater.* **2022**, *34*, 6268.
[108] a) T. Kitao, Y. Zhang, S. Kitagawa, B. Wang, T. Uemura, *Chem. Soc. Rev.* **2017**, *46*, 3108; b) S. Begum, Z. Hassan, S. Bräse, M. Tsotsalas, *Langmuir* **2020**, *36*, 10657.
[109] a) Y. R. Chiu, Y. T. Hsu, C. Y. Wu, T. H. Lin, Y. Z. Yang, H. Y. Chen, *Chem. Mater.* **2020**, *32*, 1120; b) H. Y. Tung, Z. Y. Guan, T. Y. Liu, H. Y. Chen, *Nat. Commun.* **2018**, *9*, 2564; c) C. Y. Wu, T. Y. Wu, Z. Y. Guan, P. Y. Wang, Y. C. Yang, C. W. Huang, T. H. Lin, H. Y. Chen, *Nat. Commun.* **2021**, *12*, 3413.
[110] A. Mann, M. D. Hannigan, M. Weck, *Macromol. Chem. Phys.* **2023**, *224*, 2200397.
[111] a) A. J. Blayney, I. F. Perepichka, F. Wudl, D. F. Perepichka, *Isr. J. Chem.* **2014**, *54*, 674; b) T. Junkers, J. Vandenbergh, P. Adriaensens, L. Lutsen, D. Vanderzande, *Polym. Chem.* **2012**, *3*, 275.
[112] a) H. Katayama, M. Nagao, T. Nishimura, Y. Matsui, K. Umeda, K. Akamatsu, T. Tsuruoka, H. Nawafune, F. Ozawa, *J. Am. Chem. Soc.* **2005**, *127*, 4350; b) S. Shin, M. L. Gu, C. Y. Yu, J. Jeon, E. Lee, T. L. Choi, *J. Am. Chem. Soc.* **2018**, *140*, 475; c) S. Shin, F. Menk, Y. Kim, J. Lim, K. Char, R. Zentel, T. L. Choi, *J. Am. Chem. Soc.* **2018**, *140*, 6088; d) R. M. Moslin, C. G. Espino, T. M. Swager, *Macromolecules* **2009**, *42*, 452.
[113] a) C. W. Bielawski, R. H. Grubbs, *Prog. Polym. Sci.* **2007**, *32*, 1; b) N. Zaquen, L. Lutsen, D. Vanderzande, T. Junkers, *Polym. Chem.* **2016**, *7*, 1355.
[114] Y. Yu, M. L. Turner, *Angew. Chem., Int. Ed.* **2006**, *45*, 7797.
[115] a) Y. Janpatompong, K. Suwada, M. L. Turner, G. De Bo, *Polym. Chem.* **2023**, *14*, 1978; b) Y. Janpatompong, A. M. Spring, V. Komanduri, R. U. Khan, M. L. Turner, *Macromolecules* **2022**, *55*, 10854; c) V. Komanduri, Y. Janpatompong, R. M. Hernandez, D. J. Tate, M. L. Turner, *Polym. Chem.* **2021**, *12*, 6731; d) V. Komanduri, D. R. Kumar, D. J. Tate, R. M. Hernandez, B. J. Lidster, M. L. Turner, *Polym. Chem.* **2019**, *10*, 3497; e) B. J. Lidster, S. Hirata, S. Matsuda, T. Yamamoto, V. Komanduri, D. R. Kumar, Y. Tezuka, M. Vacha, M. L. Turner, *Chem. Sci.* **2018**, *9*, 2934; f) D. R. Kumar, B. J. Lidster, R. W. Adams, M. L. Turner, *Macromolecules* **2018**, *51*, 4572; g) B. J. Lidster, J. M. Behrendt, M. L. Turner, *Chem. Commun.* **2014**, *50*, 11867; h) C. Y. Yu, M. Helliwell, J. Raftery, M. L. Turner, *Chem. - Eur. J.* **2011**, *17*, 6991; i) C. Y. Yu, M. Horie, A. M. Spring, K. Tremel, M. L. Turner, *Macromolecules* **2010**, *43*, 222; j) C. Y. Yu, J. W. Kingsley, D. G. Lidzey, M. L. Turner, *Macromol. Rapid Commun.* **2009**, *30*, 1889; k) A. M. Spring, C. Y. Yu, M. Horie, M. L. Turner, *Chem. Commun.* **2009**, 2676.
[116] F. Menk, M. Mondeshki, D. Dudenko, S. Shin, D. Schollmeyer, O. Ceyhun, T. L. Choi, R. Zentel, *Macromolecules* **2015**, *48*, 7435.
[117] a) D. R. Kumar, B. J. Lidster, R. W. Adams, M. L. Turner, *Polym. Chem.* **2017**, *8*, 3186; b) B. J. Lidster, D. R. Kumar, A. M. Spring, C. Y. Yu, M. L. Turner, *Polym. Chem.* **2016**, *7*, 5544; c) A. Mann, M. D. Hannigan, B. L. Dumlao, C. T. Hu, M. Weck, *J. Org. Chem.* **2023**, *88*, 12971.
[118] a) E. Elacqua, M. Gregor, *Angew. Chem., Int. Ed.* **2019**, *58*, 9527; b) Y. Janpatompong, V. Komanduri, R. U. Khan, M. L. Turner, *Org. Biomol. Chem.* **2023**, *21*, 3245.
[119] V. Komanduri, D. J. Tate, R. M. Hernandez, D. R. Kumar, M. L. Turner, *Macromolecules* **2019**, *52*, 7137.
[120] A. Mann, M. Weck, *ACS Macro Lett.* **2022**, *11*, 1055.
[121] a) T. W. Hsu, C. Kim, Q. Michaudel, *J. Am. Chem. Soc.* **2020**, *142*, 11983; b) S. J. Kempel, T. W. Hsu, Q. Michaudel, *Synlett* **2021**, *32*, 851; c) T. W. Hsu, S. J. Kempel, Q. Michaudel, *J. Polym. Sci.* **2022**, *60*, 569.
[122] R. K. M. Khan, S. Torker, A. H. Hoveyda, *J. Am. Chem. Soc.* **2013**, *135*, 10258.
[123] a) E. Elacqua, G. T. Geberth, D. A. Vanden Bout, M. Weck, *Chem. Sci.* **2019**, *10*, 2144; b) S. K. Pomarico, D. S. Lye, E. Elacqua, M. Weck, *Polym. Chem.* **2018**, *9*, 5655; c) E. Elacqua, M. Weck, *Chem. - Eur. J.* **2015**, *21*, 7151.
[124] A. Mann, C. Wang, B. L. Dumlao, M. Weck, *ACS Macro Lett.* **2024**, *13*, 112.
[125] Z. Pei, N. L. Magann, M. J. Sowden, R. B. Murphy, M. G. Gardiner, M. S. Sherburn, M. L. Coote, *J. Am. Chem. Soc.* **2023**, *145*, 16037.

Zahid Hassan led a research team at the Institut für Organische Chemie (IOC) and Institute of Functional Interfaces (IFG) at the Karlsruher Institüt für Technologie (KIT) in synthetic organic chemistry, materials synthesis via molecular self-assembly. He studied chemistry at HEJ Research Institute of Chemistry (M.Phil.), at the Institut für Organische Chemie, Leibniz Universität Hannover, and received Dr. rer. nat., at the Institut für Organische Chemie (Leibniz-Institut für Katalyse) Universität Rostock, Germany. After IBS Fellowship at the Centre for Self-Assembly and Complexity (CSC), Institute for Basic Sciences (IBS), POSTECH he held a faculty position at the University of Nizwa from where he moved to KIT in 2017. Significant efforts in his current research are devoted to cyclophane chemistry, exploring molecular materials via self-assembly and understanding the chemical aspects behind system-level functions.